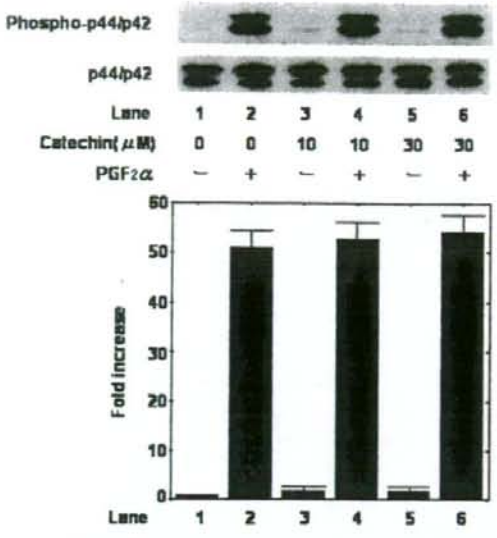

Fig. 1. Effect of EGCG on the phosphorylation of p44/p42 MAP kinase induced by $PGF_{2\alpha}$ in MC3T3-E1 cells. The cultured cells were pretreated with the indicated doses of EGCG or vehicle for 60 min, and then stimulated by 10 μM $PGF_{2\alpha}$ or vehicle for 30 min. The extracts of cells were subjected to SDS–PAGE with subsequent Western blotting analysis with antibodies against phospho-specific p44/p42 MAP kinase or p44/p42 MAP kinase. The histogram shows quantitative representations of the levels of $PGF_{2\alpha}$-induced phosphorylation obtained from laser densitometric analysis of three independent experiments. Each value represents the mean ± SEM of triplicate determinations. Similar results were obtained with two additional and different cell preparations.

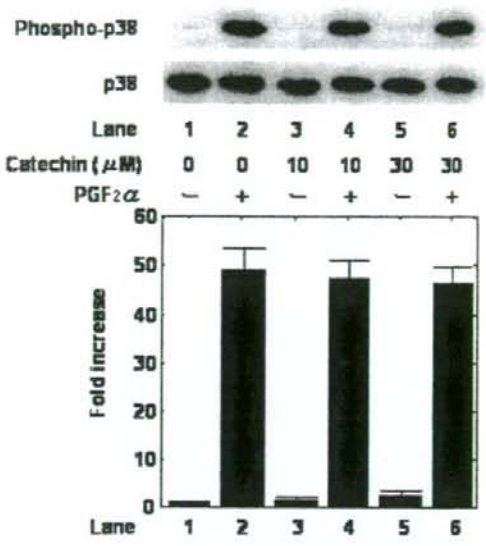

Fig. 2. Effect of EGCG on the phosphorylation of p38 MAP kinase induced by $PGF_{2\alpha}$ in MC3T3-E1 cells. The cultured cells were pretreated with the indicated doses of EGCG or vehicle for 60 min, and then stimulated by 10 μM $PGF_{2\alpha}$ or vehicle for 10 min. The extracts of cells were subjected to SDS–PAGE with subsequent Western blotting analysis with antibodies against phospho-specific p38 MAP kinase or p38 MAP kinase. The histogram shows quantitative representations of the levels of $PGF_{2\alpha}$-induced phosphorylation obtained from laser densitometric analysis of three independent experiments. Each value represents the mean ± SEM of triplicate determinations. Similar results were obtained with two additional and different cell preparations.

through p44/p42 MAP kinase activation in MC3T3-E1 cells, we next examined the effect of EGCG on the $PGF_{2\alpha}$-induced phosphorylation of p44/p42 MAP kinase. However, EGCG hardly affected the $PGF_{2\alpha}$-induced phosphorylation of p44/p42 MAP kinase (Fig. 1).

Effect $PGF_{2\alpha}$ of on the Phosphorylation of p38 MAP Kinase and SAPK/JNK in MC3T3-E1 Cells

Among the MAP kinase superfamily, p38 MAP kinase and SAPK/JNK in addition to p44/p42 MAP kinase play a crucial role as intracellular components to transduce the various signals of agonists [Widmann et al., 1999]. Therefore, in order to investigate whether activates p38 MAP kinase or SAPK/JNK in MC3T3-E1 cells, we next examined the effect of $PGF_{2\alpha}$ on the phosphorylation of p38 MAP kinase and SAPK/JNK. $PGF_{2\alpha}$ induced both the phosphorylation of p38 MAP kinase (lane 2 in Fig. 2) and SAPK/JNK (lane 2 in Fig. 3).

Effects of SB203580 or SP600125 on the $PGF_{2\alpha}$-Stimulated VEGF Synthesis in MC3T3-E1 Cells

In order to clarify the involvement of the MAP kinases in the $PGF_{2\alpha}$-stimulated VEGF synthesis in MC3T3-E1 cells, we examined the effect of SB203580, a specific inhibitor of p38 MAP kinase [Cuenda et al., 1995] or SP600125, a specific SAPK/JNK inhibitor [Bennett et al., 2001], on the VEGF synthesis. SB203580 or SP600125, which by itself had little effect on the VEGF levels, significantly suppressed the $PGF_{2\alpha}$-stimulated synthesis of VEGF (Table II).

Effect of EGCG on the Phosphorylation of p38 MAP Kinase or SAPK/JNK Induced by $PGF_{2\alpha}$ in MC3T3-E1 Cells

In order to clarify whether p38 MAP kinase is involved in EGCG effect on the $PGF_{2\alpha}$-

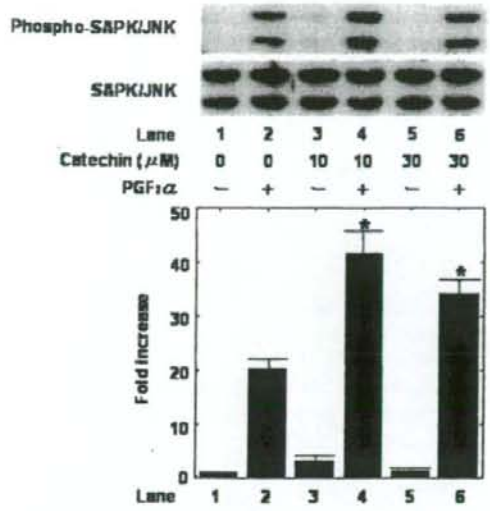

Fig. 3. Effect of EGCG on the phosphorylation of SAPK/JNK induced by $PGF_{2\alpha}$ in MC3T3-E1 cells. The cultured cells were pretreated with the indicated doses of EGCG or vehicle for 60 min, and then stimulated by 10 μM $PGF_{2\alpha}$ or vehicle for 20 min. The extracts of cells were subjected to SDS–PAGE with subsequent Western blotting analysis with antibodies against phospho-specific SAPK/JNK or SAPK/JNK. The histogram shows quantitative representations of the levels of $PGF_{2\alpha}$-induced phosphorylation obtained from laser densitometric analysis of three independent experiments. Each value represents the mean ± SEM of triplicate determinations. Similar results were obtained with two additional and different cell preparations. *$P < 0.05$, compared to the value of $PGF_{2\alpha}$ alone.

stimulated VEGF synthesis in MC3T3-E1 cells, we examined the effect of EGCG on the $PGF_{2\alpha}$-induced phosphorylation of p38 MAP kinase. However, EGCG had little effect on the $PGF_{2\alpha}$-induced phosphorylation of p38 MAP kinase (Fig. 2). On the contrary, EGCG markedly enhanced the $PGF_{2\alpha}$-induced phosphorylation of SAPK/JNK (Fig. 3). According to the densitometric analysis, EGCG (10 μM) caused about 100% enhancement of the $PGF_{2\alpha}$ effect on the SAPK/JNK phosphorylation.

TABLE II. Effects of SB203580 or SP600125 on the $PGF_{2\alpha}$-Stimulated VEGF Synthesis in MC3T3-E1 Cells

Inhibitor (μM)	$PGF_{2\alpha}$	VEGF (pg/ml)
Vehicle	–	20 ± 10
Vehicle	+	559 ± 51
SB203580 (3)	–	13 ± 10
SB203580 (3)	+	221 ± 35*
SB203580 (10)	–	15 ± 10
SB203580 (10)	+	46 ± 12*
SP600125 (1)	–	15 ± 10
SP600125 (1)	+	399 ± 37*
SP600125 (30)	–	13 ± 10
SP600125 (30)	+	162 ± 29*

The cultured cells were pretreated with SB203580, SP600125, or vehicle for 60 min, and then stimulated by 10 μM $PGF_{2\alpha}$ or vehicle for 24 h. Each value represents the mean ± SEM of triplicate determinations. Similar results were obtained with two additional and different cell preparations.
*$P < 0.05$, compared to the value of $PGF_{2\alpha}$ alone.

Effect of SP600125 on the Enhancement by EGCG of $PGF_{2\alpha}$-Induced Phosphorylation of SAPK/JNK in MC3T3-E1 Cells

SP600125 [Bennett et al., 2001], which by itself did not affect the basal levels of phosphorylation of SAPK/JNK, significantly reduced the enhancement by EGCG of $PGF_{2\alpha}$-induced SAPK/JNK phosphorylation (Fig. 4). The enhanced phosphorylation levels by EGCG of $PGF_{2\alpha}$-induced SAPK/JNK were suppressed by

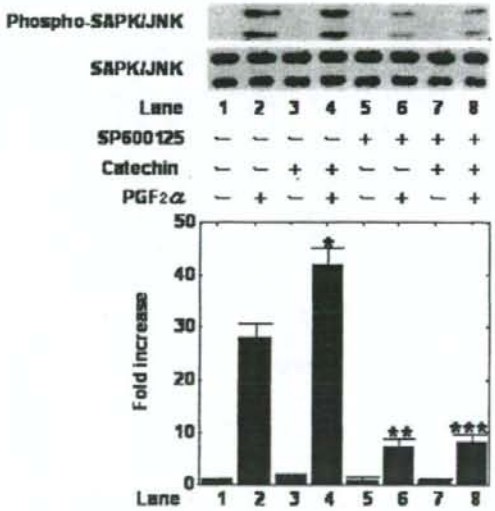

Fig. 4. Effect of SP600125 on the enhancement by EGCG of the $PGF_{2\alpha}$-induced phosphorylation of SAPK/JNK in MC3T3-E1 cells. The cultured cells were pretreated with 30 μM SP600125 or vehicle for 60 min, and then incubated by 10 μM EGCG for 60 min. The cells were stimulated by 10 μM $PGF_{2\alpha}$ or vehicle for 20 min. The extracts of cells were subjected to SDS–PAGE with subsequent Western blotting analysis with antibodies against phospho-specific SAPK/JNK or SAPK/JNK. The histogram shows quantitative representations of the levels of $PGF_{2\alpha}$-induced phosphorylation obtained from laser densitometric analysis of three independent experiments. Each value represents the mean ± SEM of triplicate determinations. Similar results were obtained with two additional and different cell preparations. *$P < 0.05$, compared to the value of $PGF_{2\alpha}$ alone. **$P < 0.05$, compared to the value of $PGF_{2\alpha}$ alone. ***$P < 0.05$, compared to the value of $PGF_{2\alpha}$ with EGCG pretreatment.

SP600125 similar to the levels by $PGF_{2\alpha}$ with SP600125 treatment.

Effect of EGCG on the Phosphorylation of c-Jun Induced by $PGF_{2\alpha}$ in MC3T3-E1 Cells

It is well known that c-Jun acts as a downstream effector of SAPK/JNK [Widmann et al., 1999; Weston and Davis, 2002]. Thus, in order to investigate whether EGCG effect on the $PGF_{2\alpha}$-stimulated VEGF synthesis is mediated through c-Jun activation in MC3T3-E1 cells, we next examined the effect of EGCG on the $PGF_{2\alpha}$-induced phosphorylation of c-Jun. We found that $PGF_{2\alpha}$ time-dependently phosphorylated c-Jun and that SP600125 suppressed the $PGF_{2\alpha}$-induced phosphorylation of c-Jun in these cells (data not shown). EGCG markedly amplified the $PGF_{2\alpha}$-induced phosphorylation of c-Jun (Fig. 5). According to the densitometric analysis, EGCG (10 μM) caused about 80% enhancement of the $PGF_{2\alpha}$ effect on the c-Jun phosphorylation.

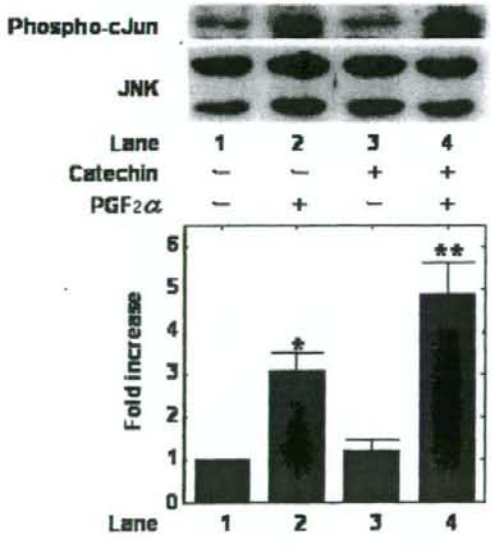

Fig. 5. Effect of EGCG on the phosphorylation of c-Jun induced by $PGF_{2\alpha}$ in MC3T3-E1 cells. The cultured cells were pretreated with the indicated doses of EGCG or vehicle for 60 min, and then stimulated by 10 μM $PGF_{2\alpha}$ or vehicle for 20 min. The extracts of cells were subjected to SDS–PAGE with subsequent Western blotting analysis with antibodies against c-Jun or SAPK/JNK. The histogram shows quantitative representations of the levels of $PGF_{2\alpha}$-induced phosphorylation obtained from laser densitometric analysis of three independent experiments. Each value represents the mean ± SEM of triplicate determinations. Similar results were obtained with two additional and different cell preparations. $^{*}P < 0.05$, compared to the control value. $^{**}P < 0.05$, compared to the value of $PGF_{2\alpha}$ alone.

DISCUSSION

In the present study, we demonstrated that EGCG, which alone did not affect the levels of VEGF, significantly enhanced the $PGF_{2\alpha}$-stimulated VEGF synthesis in osteoblast-like MC3T3-E1 cells. We next investigated the mechanism of EGCG behind the amplifying effect on the VEGF synthesis. It is well recognized that the MAP kinase superfamily mediates intracellular signaling of extracellular agonists and plays a crucial role in cellular functions including proliferation, differentiation, and cell death in a variety of cells [Widmann et al., 1999]. Three major MAP kinase, p44/p42 MAP kinase, p38 MAP kinase, and SAPK/JNK are known as central elements used by mammalian cells to transduce the diverse messages [Widmann et al., 1999]. In our previous study [Tokuda et al., 2003], we have shown that $PGF_{2\alpha}$-activated p44/p42 MAP kinase acts as a positive regulator in $PGF_{2\alpha}$-induced VEGF synthesis in osteoblast-like MC3T3-E1 cells. In the present study, we showed that EGCG failed to affect the $PGF_{2\alpha}$-induced phosphorylation of p44/p42 MAP kinase. Thus, it seems unlikely that EGCG amplifies the $PGF_{2\alpha}$-induced VEGF synthesis through upregulating the activation of p44/p42 MAP kinase in osteoblast-like MC3T3-E1 cells.

We further investigated the involvement of p38 MAP kinase and SAPK/JNK in the amplifying effect of EGCG. We found that $PGF_{2\alpha}$ induced both the phosphorylation of p38 MAP kinase and SAPK/JNK. It has been shown that MAP kinases are activated by phosphorylation of threonine and tyrosine residues by dual specificity MAP kinase kinases [Widmann et al., 1999]. Therefore, our findings strongly suggest that $PGF_{2\alpha}$ activates p38 MAP kinase and SAPK/JNK in addition to p44/p42 MAP kinase in osteoblast-like MC3T3-E1 cells. In addition, we showed that the $PGF_{2\alpha}$-stimulated VEGF synthesis was suppressed by a specific p38 MAP kinase inhibitor, SB203580 [Cuenda et al., 1995], or a specific SAPK/JNK inhibitor, SP600125 [Bennett et al., 2001]. Based on our findings, it is probable that $PGF_{2\alpha}$ stimulates the synthesis of VEGF via the three MAP kinases in osteoblast-like MC3T3-E1 cells.

However, EGCG had little effect on the $PGF_{2\alpha}$-induced p38 MAP kinase phosphorylation. Therefore, it seems unlikely that the EGCG-induced enhancement of $PGF_{2\alpha}$-stimulated VEGF synthesis is due to the upregulation of p38 MAP kinase activation. On the contrary, we showed that the $PGF_{2\alpha}$-induced SAPK/JNK phosphorylation was markedly amplified by EGCG. Furthermore, SP600125 [Bennett et al., 2001] markedly reduced the enhancement by EGCG almost to the levels of $PGF_{2\alpha}$ alone with SP600125 in the phosphorylation of SAPK/JNK. These results suggest that EGCG upregulates the $PGF_{2\alpha}$-stimulated activation of SAPK/JNK. Additionally, we demonstrated that EGCG strengthened the $PGF_{2\alpha}$-induced phosphorylation of c-Jun, well known as a downstream effector of SAPK/JNK [Widmann et al., 1999; Weston and Davis, 2002], as well as SAPK/JNK. Taking our findings into account as a whole, it is most likely that EGCG upregulates $PGF_{2\alpha}$-stimulated VEGF synthesis through enhancing the activation of SAPK/JNK in osteoblast-like MC3T3-E1 cells. Further investigations are necessary to clarify the precise mechanism of catechin behind the amplification of VEGF synthesis in osteoblasts.

It is generally recognized that the expansion of capillary network providing microvasculature is an essential process of bone remodeling [Erlebacher et al., 1995]. Since VEGF is a specific mitogen of vascular endothelium [Ferrara and Davis-Smyth, 1997], it is speculated that VEGF synthesized by osteoblasts functions as a pivotal intercellular mediator between osteoblasts and vascular endothelial cells. Moreover, it has been reported that VEGF is involved in trabecular bone formation and expansion of the hypertrophic chondrocyte zone in epiphyseal growth plate of mouse [Gerber et al., 1999], supporting the importance of VEGF in bone metabolism. On the other hand, it has been shown that catechin exerts an inhibitory effect on bone resorption [Delaisse et al., 1986]. Additionally, in osteoblasts, production of bone-resorptive cytokines such as tumor necrosis factor-α and interleukin-6 has been reported to be suppressed by catechin [Choi and Hwang, 2003]. Based on our results as a whole, it is probable that catechin-enhanced VEGF synthesized from osteoblasts acts a crucial role in the process of bone remodeling via regulating the capillary endothelial cells proliferation. Further investigations are required to elucidate the role of catechin in bone metabolism.

In conclusion, our present results strongly suggest that catechin upregulates $PGF_{2\alpha}$-stimulated VEGF synthesis via enhancing activation of SAPK/JNK among the MAP kinase superfamily in osteoblasts.

ACKNOWLEDGMENTS

We are very grateful to Yoko Kawamura and Seiko Sakakibara for their skillful technical assistance.

REFERENCES

Bennett BL, Sasaki DT, Murray BW, O'Leary EC, Sakata ST, Xu W, Leisten JC, Motiwala A, Pierce S, Satoh Y, Bhagwat SS, Manning AM, Anderson DW. 2001. SP600125, an anthrapyrazolone inhibitor of Jun N-terminal Kinase. Proc Natl Acad Sci USA 98:13681–13686.

Choi E-M, Hwang J-K. 2003. Effects of (+)-catechin on the function of osteoblastic cells. Biol Pharm Bull 26:523–526.

Cuenda A, Rouse J, Doza YN, Meier R, Cohen P, Gallagher TF, Young PR, Lee JC. 1995. SB203580 is a specific inhibitor of a MAP kinase homologue which is stimulated by cellular stresses and interleukin-1. FEBS Lett 364:229–233.

Delaisse JM, Eeckhout Y, Vaes G. 1986. Inhibition of bone resorption in culture by (+)-catechin. Biochem Pharmacol 35:3091–3094.

Erlebacher A, Filvaroff EH, Girelman SE, Derynck R. 1995. Toward a molecular understanding of skeletal development. Cell 80:371–378.

Exton JH. 1999. Regulation of phospholipase D. Biochim Biophys Acta 439:121–133.

Ferrara N, Davis-Smyth T. 1997. The biology of vascular endothelial growth factor. Endocr Rev 18:4–25.

Gerber HP, Vu TH, Ryan AM, Kowalski J, Werb Z, Ferrara N. 1999. VEGF couples hypertrophic cartilage remodeling, ossification and angiogenesis during endochondral bone formation. Nat Med 5:623–628.

Goad DL, Rubin J, Wang H, Jr., Tashijian AH, Patterson C. 1996. Enhanced expression of vascular endothelial growth factor in human SaOS-2 osteoblast-like cells and murine osteoblasts induced by insulin-like growth factor I. Endocrinology 137:2262–2268.

Harbourne JB, Williams CA. 2000. Advances in flavonoid research since 1992. Phytochemistry 55:481–504.

Jankun J, Selman SH, Swiercz R, Skrzypczak-Jankun E. 1997. Why drinking green tea could prevent cancer. Nature 387:561.

Kato K, Ito H, Hasegawa K, Inaguma Y, Kozawa O, Asano T. 1996. Modulation of the stress-induced synthesis of hsp27 and αB-crystallin by cyclic AMP in C6 glioma cells. J Neurochem 66:946–950.

Kozawa O, Tokuda H, Miwa M, Kotoyori J, Oiso Y. 1992. Cross-talk regulation between cyclic AMP production and phosphoinositide hydrolysis induced by prostaglandin E_2 in osteoblast-like cells. Exp Cell Res 198:130–134.

Kozawa O, Suzuki A, Kotoyori J, Tokuda H, Watanabe Y, Ito Y, Oiso Y. 1994. Prostaglandin $F_{2\alpha}$ activates phospholipase D independently from activation of protein kinase C in osteoblast-like cells. J Cell Biochem 55:373–379.

Laemmli UK. 1970. Cleavage of structural proteins during the assembly of the head of bacteriophage T4. Nature 227:680–685.

Miwa M, Tokuda H, Tsushita K, Kotoyori J, Takahashi Y, Ozaki N, Kozawa O, Oiso Y. 1990. Involvement of pertussis toxin-sensitive GTP-binding protein in prostaglandin $F_{2\alpha}$-induced phosphoinositide hydrolysis in osteoblast-like cells. Biochem Biophys Res Commun 171:1229–1235.

Nijweide PJ, Burger EH, Feyen JHM. 1986. Cells of bone: Proliferation, differentiation and hormonal regulation. Physiol Rev 66:855–886

Nishizuka Y. 1992. Intracellular signaling by hydrolysis of phospholipids and activation of protein kinase C. Science 258:607–614.

Pilbeam CC, Harrison JR, Raisz LG. 1996. Prostaglandins and bone metabolism. In: Bilezikian JP, Raisz LG, Rodan GA, editors. Principles of bone biology. San Diego: Academic Press. pp 715–728.

Schalaeppi JM, Gutzwiller S, Finlenzeller G, Fournier B. 1997. 1,25-dihydroxyvitamin D_3 induces the expression of vascular endothelial growth factor in osteoblastic cells. Endocr Res 23:213–229.

Sudo H, Kodama H, Amagai Y, Yamamoto S, Kasai S. 1983. *In vivo* differentiation and calcification in a new clonal osteogenic cell line derived from newborn mouse calvaria. J Cell Biol 96:191–198.

Tokuda H, Harada A, Hirade K, Matsuno H, Ito H, Kato K, Oiso Y, Kozawa O. 2003. Incadronate amplifies prostaglandin $F_{2\alpha}$-induced vascular endothelial growth factor synthesis in osteoblasts. Enhancement of MAPK activity. J Biol Chem 278:18930–18937.

Wang DS, Yamazaki K, Nohtomi K, Shizume K, Ohsumi K, Shibuya M, Demura H, Sato K. 1996. Increase of vascular endothelial growth factor mRNA expression by 1,25-dihydroxyvitamin D_3 in human osteoblast-like cells. J Bone Miner Res 11:472–479.

Weston CR, Davis RJ. 2002. The JNK signal transduction pathway. Curr Opin Genet Dev 12:14–21.

Widmann C, Gibson S, Jarpe MB, Johnson GL. 1999. Mitogen-activated protein kinase: Conservation of a three-kinase module from yeast to human. Physiol Rev 79:143–180.

FEBS Letters 581 (2007) 1311–1316

(−)-Epigallocatechin gallate suppresses endothelin-1-induced interleukin-6 synthesis in osteoblasts: Inhibition of p44/p42 MAP kinase activation

Haruhiko Tokuda[a,b,*], Shinji Takai[b], Yoshiteru Hanai[a,b], Rie Matsushima-Nishiwaki[b], Takayuki Hosoi[c], Atsushi Harada[d], Toshiki Ohta[e], Osamu Kozawa[b]

[a] *Department of Clinical Laboratory, National Hospital for Geriatric Medicine, National Center for Geriatrics and Gerontology, Obu 474-8511, Japan*
[b] *Department of Pharmacology, Gifu University Graduate School of Medicine, Gifu 501-1194, Japan*
[c] *Department of Advanced Medicine, National Hospital for Geriatric Medicine, National Center for Geriatrics and Gerontology, Obu 474-8511, Japan*
[d] *Department of Restorative Medicine, National Hospital for Geriatric Medicine, National Center for Geriatrics and Gerontology, Obu 474-8511, Japan*
[e] *Department of Internal Medicine, National Hospital for Geriatric Medicine, National Center for Geriatrics and Gerontology, Obu 474-8511, Japan*

Received 17 February 2007; accepted 22 February 2007

Available online 1 March 2007

Edited by Beat Imhof

Abstract **We previously showed that endothelin-1 (ET-1) stimulates the synthesis of interleukin-6 (IL-6), a potent bone resorptive agent, in osteoblast-like MC3T3-E1 cells, and that protein kinase C (PKC)-dependent p44/p42 mitogen-activated protein (MAP) kinase plays a part in the IL-6 synthesis. In the present study, we investigated the effect of (−)-epigallocatechin gallate (EGCG), one of the major flavonoids containing in green tea, on ET-1-induced IL-6 synthesis in osteoblasts and the underlying mechanism. EGCG significantly reduced the synthesis of IL-6 stimulated by ET-1 in MC3T3-E1 cells as well primary cultured mouse osteoblasts. SB203580, a specific inhibitor of p38 MAP kinase, but not SP600125, a specific SAPK/JNK inhibitor, suppressed ET-1-stimulated IL-6 synthesis. ET-1-induced phosphorylation of p38 MAP kinase was not affected by EGCG. On the other hand, EGCG suppressed the phosphorylation of p44/p42 MAP kinase induced by ET-1. Both the IL-6 synthesis and the phosphorylation of p44/p42 MAP kinase stimulated by 12-*O*-tetradecanoylphorbol 13-acetate (TPA), a direct activator of PKC, were markedly suppressed by EGCG. The phosphorylation of MEK1/2 and Raf-1 induced by ET-1 or TPA were also inhibited by EGCG. These results strongly suggest that EGCG inhibits ET-1-stimulated synthesis of IL-6 via suppression of p44/p42 MAP kinase pathway in osteoblasts, and the inhibitory effect is exerted at a point between PKC and Raf-1 in the ET-1 signaling cascade.**

Keywords: Catechin; Endothelin-1; Interleukin-6; MAP kinase; Osteoblast

1. Introduction

Interleukin-6 (IL-6) is a pleiotropic cytokine that has important physiological effects on a wide range of functions such as promoting B cell differentiation, T cell activation and inducing acute phase proteins [1–4]. The bone metabolism is regulated by two functional cells, osteoblasts and osteoclasts, responsible for bone formation and bone resorption, respectively [5]. The formation of bone structures and bone remodeling results from the coupling process, bone resorption by activated osteoclasts with subsequent deposition of new matrix by osteoblasts. It is well recognized that IL-6 is one of the most potent osteoclastogenic factors in the bone metabolism [3,4]. Bone resorption is mediated by the increased local production of inflammatory cytokines such as tumor necrosis factor-α and IL-1. In osteoblasts [6–8], bone resorptive agents such as tumor necrosis factor-α and IL-1 have been reported to stimulate the synthesis of IL-6. As for the bone metabolism, IL-6 has been shown to stimulate bone resorption and induce osteoclast formation [3,4,6,9]. Therefore, accumulating evidence indicates that IL-6 secreted from osteoblasts plays a key role as a downstream effector of bone resorptive agents. In previous studies [10,11], we have shown that endothelin-1 (ET-1) induces the activation of p44/p42 mitogen-activated protein (MAP) kinase, a member of the MAP kinase superfamily [12], via protein kinase C (PKC), resulting in the IL-6 synthesis in osteoblast-like MC3T3-E1 cells. However, the mechanism of ET-1 behind the IL-6 synthesis in osteoblasts has not yet been precisely clarified.

It is well known that compounds in foods such as vegetables and fruits have beneficial properties on human beings. Among them, it has been reported that flavonoids possess antioxidative, antibacterial and antitumor effects [13,14]. Catechins are one of the major flavonoids, which are present in various species of plants such as green tea [14]. In bone metabolism, catechin has been shown to suppress bone resorption [15]. As for osteoblasts, it has been shown that catechin stimulates alkaline phosphatase activity, a mature osteoblast phenotype [5], and reduces apoptosis in osteoblast-like MC3T3-E1 cells [16]. However, the precise mechanism of catechin in osteoblasts is not fully known.

In the present study, we investigated whether (−)-epigallocatechin gallate (EGCG), one of the major flavonoids containing in green tea, affects the ET-1-stimulated IL-6 synthesis in osteoblast-like MC3T3-E1 cells and the mechanism behind it. We herein show that EGCG reduces the ET-1-stimulated

*Corresponding author. Address: Department of Clinical Laboratory, National Hospital for Geriatric Medicine, National Center for Geriatrics and Gerontology, Obu 474-8511, Japan.
Fax: +81 562 46 8396.
E-mail address: tokuda@ncgg.go.jp (H. Tokuda).

0014-5793/$32.00
doi:10.1016/j.febslet.2007.02.052

IL-6 synthesis via attenuation of p44/p42 MAP kinase pathway in these cells.

2. Materials and methods

2.1. Materials

ET-1 and 12-*O*-tetradecanoylphorbol 13-acetate (TPA) were purchased from Sigma Chemical Co. (St. Louis, MO). IL-6 ELISA kit was purchased from R&D Systems, Inc. (Minneapolis, MN). EGCG, SB203580 and SP600125 were obtained from Calbiochem-Novabiochem Co. (La Jolla, CA). Phospho-specific p38 MAP kinase antibodies, p38 MAP kinase antibodies, phospho-specific p44/p42 MAP kinase antibodies, p44/p42 MAP kinase antibodies, phospho-specific MEK1/2 antibodies, MEK1/2 antibodies, phospho-specific Raf-1 antibodies and β-actin antibodies were purchased from Cell Signaling Technology (Beverly, MA). ECL Western blotting detection system was purchased from Amersham Japan (Tokyo, Japan). Other materials and chemicals were obtained from commercial sources. SB203580 and SP600125 were dissolved in dimethyl sulfoxide. The maximum concentration of dimethyl sulfoxide was 0.1%, which did not affect either the assay for IL-6 activity or the Western blotting analysis.

2.2. Cell culture

The cloned osteoblast-like MC3T3-E1 cells, which have been derived from newborn mouse calvaria [17], were maintained as previously described [18]. Briefly, the cells were cultured in α-minimum essential medium (α-MEM) containing 10% fetal calf serum (FCS) at 37 °C in a humidified atmosphere of 5% CO_2/95% air. The cells were seeded into 35-mm diameter dishes (5×10^4/dish) or 90-mm diameter dishes (5×10^5/dish) in α-MEM containing 10% FCS. After 5 days, the medium was exchanged for α-MEM containing 0.3% FCS. The cells were used for experiments after 48 h.

Primary cultured mouse osteoblasts were obtained from neonatal balb/c mouse by sequential collagenase digestions as previously described [19]. In brief, the calvarias of the neonatal mice were aseptically dissected from neonatal mice. The calvarias which were divided into small pieces were sequentially digested with 5 ml of PBS containing 0.1% collagenase (Sigma, MO) for 5 min at 37 °C. The cells isolated in fractions 2–6 were seeded into 90-mm diameter dishes in α-MEM containing 10% FCS at 37 °C in a humidified atmosphere of 5% CO_2/95% air. The medium was exchanged at every 3 days. After reaching confluence, the cells were subcultured. After trypsinization using trypsin-EDTA (0.05%/0.53 mM), the cells were rinsed three times in 10 ml of PBS. The cells (1×10^5) were seeded into 35-mm diameter dishes in 2 ml of α-MEM containing 10% FCS. After reaching confluency, the medium was exchanged for α-MEM containing 0.3% FCS. The cells were used for experiments after 48 h. We confirmed that the cultured cells possessed the high alkaline phosphatase activity, a mature osteoblasts phenotype [20].

2.3. Assay for IL-6

The cultured cells were stimulated by ET-1 in 1 ml of α-MEM containing 0.3% FCS, and then incubated for the indicated periods. The conditioned medium was collected, and IL-6 in the medium was then measured by an IL-6 ELISA kit. When indicated, the cells were pretreated with EGCG, SB203580 or SP600125 for 60 min.

2.4. Analysis of Western blotting

The cultured cells were stimulated by ET-1 in α-MEM containing 0.3% FCS for the indicated periods. The cells were washed twice with phosphate-buffered saline and then lysed, homogenized and sonicated in a lysis buffer containing 62.5 mM Tris/HCl, pH 6.8, 2% sodium dodecyl sulfate (SDS), 50 mM dithiothreitol and 10% glycerol. The cytosolic fraction was collected as a supernatant after centrifugation at $125000 \times g$ for 10 min at 4 °C. SDS–polyacrylamide gel electrophoresis (PAGE) was performed by Laemmli [21] in 10% polyacrylamide gel. A Western blotting analysis was performed as described previously [22] by using phospho-specific p38 MAP kinase antibodies, p38 MAP kinase antibodies, phospho-specific p44/p42 MAP kinase or p44/p42 MAP kinase with peroxidase-labeled antibodies raised in goat against rabbit IgG being used as second antibodies. The peroxidase activity on PVDG membrane was visualized on X-ray film by means of the ECL Western blotting detection system. When indicated, the cells were pretreated with various doses of EGCG for 60 min.

2.5. Determinations

The absorbance of enzyme immunoassay samples was measured at 450 nm with EL 340 Bio Kinetic Reader (Bio-Tek Instruments, Inc., Winooski, VT). A densitometric analysis was performed using the Molecular Analyst/Macintosh software program (Bio-Rad Laboratories, Hercules, CA).

2.6. Statistical analysis

The data were analyzed by ANOVA followed by the Bonferroni method for multiple comparisons between pairs, and a $P < 0.05$ was considered significant. All data are presented as the means ± S.E.M. of triplicate determinations. Each experiment was repeated three times with similar results.

3. Results

3.1. Effects of EGCG on the ET-1-stimulated IL-6 synthesis in MC3T3-E1 cells and primary cultured mouse osteoblasts

We have previously demonstrated that ET-1 stimulates IL-6 synthesis in osteoblast-like MC3T3-E1 cells [10]. We first examined the effect of EGCG on the ET-1-stimulated IL-6 synthesis. EGCG, which alone had little effect on the IL-6 levels, reduced the ET-1-stimulated synthesis of IL-6 in a dose-dependent manner in the range between 1 and 100 μM (Table 1). In addition, we also examined the effect of EGCG in primary cultured mouse osteoblasts, and found that EGCG (30 μM) significantly reduced the IL-6 synthesis induced by ET-1 (Table 2). EGCG (30 μM) caused about a 55% reduction in the ET-1-effect.

3.2. Effects of SB203580 or SP600125 on the ET-1-stimulated IL-6 synthesis in MC3T3-E1 cells

In our previous study [11], we reported that p44/p42 MAP kinase plays a part in the ET-1-stimulated IL-6 synthesis in MC3T3-E1 cells. Among the MAP kinase superfamily, p38

Table 1
Effects of EGCG, SB203580 or SP600125 on the ET-1-stimulated IL-6 synthesis in MC3T3-E1 cells

EGCG or inhibitor	ET-1	IL-6 (pg/ml)
Vehicle	–	16 ± 5
Vehicle	+	468 ± 38*
EGCG (1 μM)	–	15 ± 10
EGCG (1 μM)	+	419 ± 35
EGCG (10 μM)	–	17 ± 8
EGCG (10 μM)	+	414 ± 30
EGCG (50 μM)	–	15 ± 10
EGCG (50 μM)	+	347 ± 28**
EGCG (100 μM)	–	23 ± 8
EGCG (100 μM)	+	69 ± 12**
SB203580	–	10 ± 7
SB203580	+	85 ± 12**
SP600125	–	15 ± 10
SP600125	+	456 ± 29

The cultured cells were pretreated with various doses of EGCG, 10 μM SB203580, 10 μM SP600125 or vehicle for 60 min, and then stimulated by 0.1 μM ET-1 or vehicle for 24 h. Each value represents the means ± S.E.M. of triplicate determinations. Similar results were obtained with two additional and different cell preparations.
*$P < 0.05$, compared to the control value.
**$P < 0.05$, compared to the value of ET-1 alone.

Table 2
Effects of EGCG on the ET-1-stimulated IL-6 synthesis in primary cultured mouse osteoblasts

EGCG	ET-1	IL-6 (pg/ml)
–	–	248 ± 39
–	+	354 ± 26*
+	–	216 ± 8
+	+	263 ± 26**

The cultured cells were pretreated with 30 μM EGCG or vehicle for 60 min, and then stimulated by 0.1 μM ET-1 or vehicle for 24 h. Each value represents the means ± S.E.M. of triplicate determinations. Similar results were obtained with two additional and different cell preparations.
*$P < 0.05$, compared to the control value.
**$P < 0.05$, compared to the value of ET-1 alone.

MAP kinase and stress-activated protein kinase (SAPK)/c-Jun N-terminal kinase (JNK) in addition to p44/p42 MAP kinase, which together play a crucial role as intracellular components to transduce the various signals of agonists [12]. We have previously shown that ET-1 also activates p38 MAP kinase and SAPK/JNK [23,24]. In order to clarify the involvement of the MAP kinases in the ET-1-stimulated IL-6 synthesis in these cells, we examined the effect of SB203580, a specific inhibitor of p38 MAP kinase [25], or SP600125, a specific SAPK/JNK inhibitor [26], on the IL-6 synthesis. SB203580, which by itself had little effect on the IL-6 levels, significantly suppressed the ET-1-stimulated synthesis of IL-6 (Table 1). On the other hand, SP600125 hardly affected the IL-6 synthesis induced by ET-1 (Table 1).

3.3. Effect of EGCG on the phosphorylation of p38 MAP kinase by ET-1 in MC3T3-E1 cells

In order to clarify whether p38 MAP kinase is involved in EGCG-effect on the ET-1-stimulated IL-6 synthesis in MC3T3-E1 cells, we examined the effect of EGCG on the ET-1-induced phosphorylation of p38 MAP kinase. However, EGCG had little effect on the ET-1-induced phosphorylation of p38 MAP kinase (Fig. 1).

3.4. Effect of EGCG on the phosphorylation of p44/p42 MAP kinase induced by ET-1 in MC3T3-E1 cells

In order to investigate whether EGCG-effect on the ET-1-stimulated IL-6 synthesis is mediated through p44/p42 MAP kinase activation in MC3T3-E1 cells, we next examined the effect of EGCG on the ET-1-induced phosphorylation of p44/p42 MAP kinase. EGCG markedly attenuated the ET-1-induced phosphorylation of p44/p42 MAP kinase (Fig. 2). According to the densitometric analysis, EGCG (100 μM) caused about 80% reduction in the ET-1-effect.

3.5. Effects of EGCG on the TPA-stimulated IL-6 synthesis in MC3T3-E1 cells

We previously reported that PKC functions at a point upstream from p44/p42 MAP kinase in the ET-1-stimulated IL-6 synthesis in osteoblast-like MC3T3-E1 cells [11]. We next examined the effect of EGCG on the IL-6 synthesis stimulated by TPA, a direct activator of PKC [27]. In our previous study [28], we found that TPA alone stimulates IL-6 synthesis in MC3T3-E1 cells. EGCG, which by itself had little effect on the IL-6 levels, significantly reduced the TPA-stimulated synthesis of IL-6 (Table 3). EGCG (100 μM) caused about an 80% reduction in the TPA-effect.

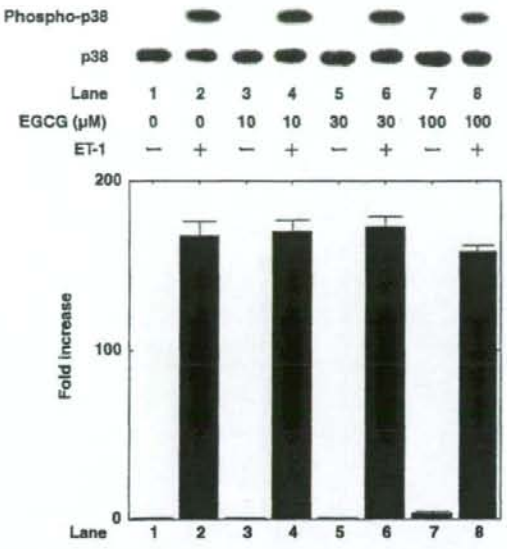

Fig. 1. Effect of EGCG on the phosphorylation of p38 MAP kinase induced by ET-1 in MC3T3-E1 cells. The cultured cells were pretreated with the indicated doses of EGCG or vehicle for 60 min, and then stimulated by 3 nM ET-1 or vehicle for 20 min. The extracts of cells were subjected to SDS–PAGE with a subsequent Western blotting analysis with antibodies against phospho-specific p38 MAP kinase or p38 MAP kinase. The histogram shows quantitative representations of the levels of ET-1-induced phosphorylation obtained from a laser densitometric analysis of three independent experiments. Each value represents the means ± S.E.M. of triplicate determinations. Similar results were obtained with two additional and different cell preparations.

3.6. Effect of EGCG on the phosphorylation of p44/p42 MAP kinase induced by TPA in MC3T3-E1 cells

In order to investigate whether EGCC-effect on the TPA-stimulated IL-6 synthesis is mediated through inhibition of p44/p42 MAP kinase activation in MC3T3-E1 cells, we next examined the effect of EGCC on the TPA-induced phosphorylation of p44/p42 MAP kinase. We previously found that TPA induces the phosphorylation of p44/p42 MAP kinase in these cells [29]. EGCC markedly suppressed the TPA-induced phosphorylation of p44/p42 MAP kinase (Fig. 3).

3.7. Effects of EGCG on the phosphorylation of MEK1/2 and Raf-1 induced by ET-1 or TPA in MC3T3-E1 cells

It is well known that p44/p42 MAP kinase is activated by an upstream kinase, MEK1/2, which is activated by Raf-1 [12]. To clarify the exact mechanism of EGCG behind the IL-6 synthesis, we further examined the effects of EGCG on the phosphorylation of MEK1/2 and Raf-1 induced by ET-1 or TPA in MC3T3-E1 cells. The levels of ET-1 or TPA-induced phosphorylation of MEK1/2 were reduced by EGCG (data not shown). EGCG suppressed the levels of both ET-1- and TPA-induced the phosphorylation of Raf-1 (Fig. 4).

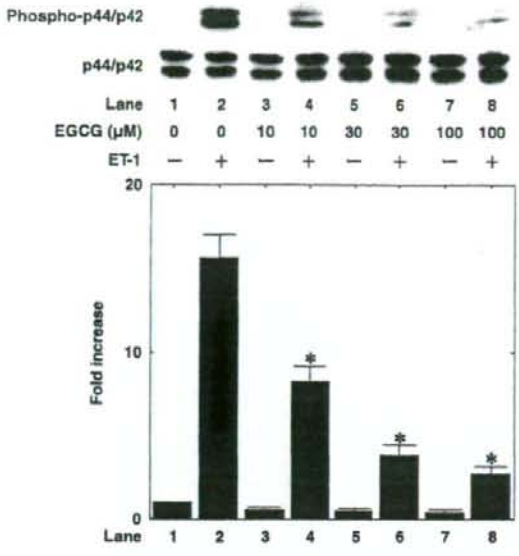

Fig. 2. Effect of EGCG on the phosphorylation of p44/p42 MAP kinase induced by ET-1 in MC3T3-E1 cells. The cultured cells were pretreated with the indicated doses of EGCG or vehicle for 60 min, and then stimulated by 3 nM ET-1 or vehicle for 5 min. The extracts of the cells were subjected to SDS–PAGE with a subsequent Western blotting analysis with antibodies against phospho-specific p44/p42 MAP kinase or p44/p42 MAP kinase. The histogram shows quantitative representations of the levels of ET-1-induced phosphorylation obtained from a laser densitometric analysis of three independent experiments. Each value represents the means ± S.E.M. of triplicate determinations. Similar results were obtained with two additional and different cell preparations. $^{*}P < 0.05$, compared to the value of ET-1 alone.

Table 3
Effect of EGCG on the TPA-stimulated IL-6 synthesis in MC3T3-E1 cells

EGCG	TPA	IL-6 (pg/ml)
–	–	19 ± 7
–	+	415 ± 31*
+	–	29 ± 10
+	+	98 ± 17**

The cultured cells were pretreated with 100 μM EGCG or vehicle for 60 min, and then stimulated by 0.1 μM TPA or vehicle for 24 h. Each value represents the means ± S.E.M. of triplicate determinations. Similar results were obtained with two additional and different cell preparations.
*$P < 0.05$, compared to the control value.
**$P < 0.05$, compared to the value of TPA alone.

4. Discussion

In the present study, we showed that EGCG, which by itself had little effect on the levels of IL-6, significantly reduced the ET-1-stimulated IL-6 synthesis in osteoblast-like MC3T3-E1 cells. We found that EGCG reduced the IL-6 synthesis induced by ET-1 also in primary cultured mouse osteoblasts. It is likely that the inhibitory effect of EGCG on the IL-6 synthesis induced by ET-1 is not specific in a clonal osteoblast-like

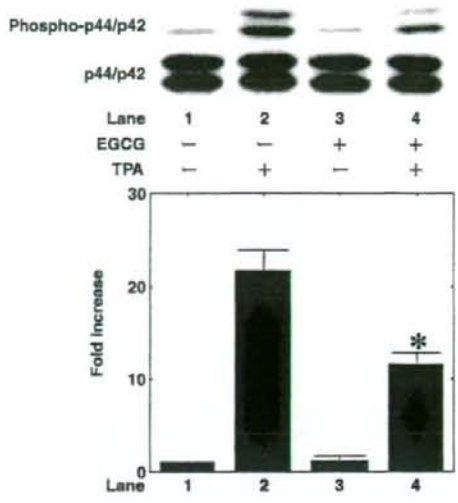

Fig. 3. Effect of EGCG on the phosphorylation of p44/p42 MAP kinase induced by TPA in MC3T3-E1 cells. The cultured cells were pretreated with 100 μM EGCG or vehicle for 60 min, and then stimulated by 0.1 μM TPA or vehicle for 60 min. The extracts of cells were subjected to SDS–PAGE with a subsequent Western blotting analysis with antibodies against phospho-specific p44/p42 MAP kinase or p44/p42 MAP kinase. The histogram shows quantitative representations of the levels of TPA-induced phosphorylation obtained from a laser densitometric analysis of three independent experiments. Each value represents the means ± S.E.M. of triplicate determinations. Similar results were obtained with two additional and different cell preparations. $^{*}P < 0.05$, compared to the value of TPA alone.

MC3T3-E1 cells but it is common in osteoblasts. We next investigated the mechanism of EGCG underlying the suppressive effect on the IL-6 synthesis. It is generally known that the MAP kinase superfamily plays a pivotal role in cellular functions including proliferation, differentiation, and cell death in a variety of cells [12]. Three major MAP kinase, p44/p42 MAP kinase, p38 MAP kinase, and SAPK/JNK are known as central elements used by mammalian cells to transduce the diverse messages [12]. We have previously reported that ET-1-activated p44/p42 MAP kinase acts as a positive regulator in ET-1-induced IL-6 synthesis in osteoblast-like MC3T3-E1 cells [11]. In addition, we demonstrated that p38 MAP kinase and SAPK/JNK are activated by ET-1 in these cells [23,24]. In the present study, we showed that SB203580 [25], markedly suppressed the ET-1-induced IL-6 synthesis while SP600125 [26], failed to affect the IL-6 synthesis. We previously showed that ET-1-induced both synthesis of vascular endothelial growth factor and phosphorylation of SAPK/JNK are significantly suppressed by 10 μM SP600125 in MC3T3-E1 cells [24]. It thus seems unlikely that SAPK/JNK is involved in the ET-1-induced IL-6 synthesis in osteoblast-like MC3T3-E1 cells. Based on our results, it is probable that ET-1 stimulates the synthesis of IL-6 via p38 MAP kinase in addition to p44/p42 MAP kinase in osteoblast-like MC3T3-E1 cells.

We further investigated the involvement of p38 MAP kinase and p44/p42 MAP kinase in the inhibitory effect of EGCG on the IL-6 synthesis. EGCG attenuated the ET-1-induced phosphorylation of p44/p42 MAP kinase without affecting the p38 MAP kinase phosphorylation. Therefore, our findings strongly

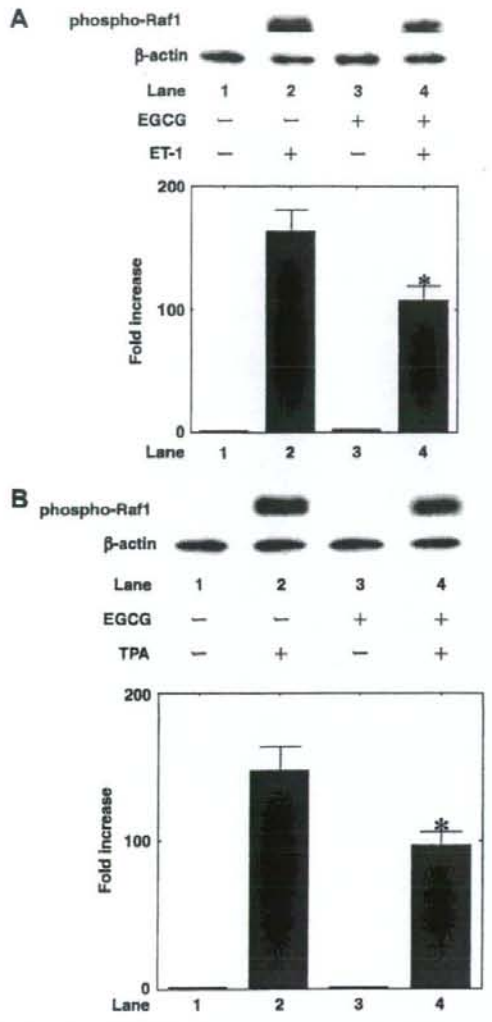

Fig. 4. Effects of EGCG on the phosphorylation of Raf-1 induced by ET-1 or TPA in MC3T3-E1 cells. The cultured cells were pretreated with 100 μM EGCG or vehicle for 60 min, and then stimulated by 0.1 μM ET-1 (A), 0.1 μM TPA (B) or vehicle for 60 min. The extracts of cells were subjected to SDS–PAGE with a subsequent Western blotting analysis with antibodies against phospho-specific Raf-1 or β-actin. The histogram shows quantitative representations of the levels of ET-1- (A) or TPA-induced phosphorylation (B) obtained from a laser densitometric analysis of three independent experiments. Each value represents the means ± S.E.M. of triplicate determinations. Similar results were obtained with two additional and different cell preparations. $^{*}P < 0.05$, compared to the value of ET-1 (A) or TPA (B) alone.

suggest that EGCG inhibits the ET-1-induced IL-6 synthesis via the down-regulating p44/p42 MAP kinase pathway in osteoblast-like MC3T3-E1 cells. In our previous studies [10,11], we demonstrated that p44/p42 MAP kinase acts at a point downstream of PKC in ET-1-stimulated IL-6 synthesis in MC3T3-E1 cells. To clarify whether the effect of catechin is exerted at a point downstream of PKC or not, we additionally examined the effect of EGCG on the IL-6 synthesis by TPA [27]. We have found that TPA alone stimulates IL-6 synthesis in MC3T3-E1 cells [28]. We herein presented that EGCG reduced the TPA-stimulated IL-6 synthesis as well as the TPA-induced phosphorylation of p44/p42 MAP kinase in these cells, suggesting that the effect of EGCG is exerted at a point upstream of p44/p42 MAP kinase. Furthermore, we found that EGCG actually suppressed the levels of both ET-1- and TPA-induced phosphorylation of MEK1/2 and Raf-1. Taking our findings into account as a whole, it is most likely that EGCG down-regulates ET-1-stimulated IL-6 synthesis in osteoblasts, and that the effect is exerted at a point between PKC and Raf-1. Further investigations are necessary to clarify the precise mechanism of catechin underlying the down-regulation of IL-6 synthesis in osteoblasts.

IL-6 is well recognized to be a potent bone resorptive agent and induces osteoclast formation [4,6]. On the other hand, catechin reportedly has an inhibitory effect on bone resorption [15]. In addition, it has recently been shown that catechin increases cell viability and alkaline phosphatase activity, a marker of mature osteoblast phenotype [5], in osteoblast-like MC3T3-E1 cells and apoptosis of these cells is suppressed by catechin [16]. Taking our results into account, it is probable that catechin-induced suppression of p44/p42 MAP kinase activation plays an effect against bone resorption via down-regulating IL-6 synthesis in osteoblasts. Our present data therefore provide new insight into the pharmacological effects of catechin action on bone cells. Further investigations are required to elucidate the exact role of catechin in the bone metabolism.

In conclusion, these results strongly suggest that catechin inhibits the ET-1-stimulated synthesis of IL-6 via suppression of p44/p42 MAP kinase pathway in osteoblasts, and this effect is exerted at a point between PKC and Raf-1 in the ET-1 signaling cascade.

Acknowledgements: We are very grateful to Yoko Kawamura and Seiko Sakakibara for their skillful technical assistance. This investigation was supported in part by Grant-in-Aid for Scientific Research (16590873 and 16591482) for the Ministry of Education, Science, Sports and Culture of Japan, the Research Grants for Longevity Sciences (15A-1, 15C-2 and 17A-3), Research Grant on Proteomics and Research Grant on Fracture and Dimentia from the Ministry of Health, Labour and Welfare of Japan.

References

[1] Akira, S., Taga, T. and Kishimoto, T. (1993) Interleukin-6 in biology and medicine. Adv. Immunol. 54, 1–78.
[2] Heymann, D. and Rousselle, A.V. (2000) gp130 Cytokine family and bone cells. Cytokine 12, 455–1468.
[3] Kwan Tat, S., Padrines, M., Theoleyre, S., Heymann, D. and Fortun, Y. (2004) IL-6, RANKL, ET-1-alpha/IL-1: interrelations in bone resorption pathophysiology. Cytokine Growth Factor Rev. 15, 49–60.
[4] Blair, H.C., Robinson, L.J. and Zaidi, M. (2005) Osteoclast signalling pathways. Biochem. Biophys. Res. Commun. 328, 728–738.
[5] Nijweide, P.J., Burger, E.H. and Feyen, J.H.M. (1986) Cells of bone: proliferation, differentiation, and humoral regulation. Physiol. Rev. 66, 855–886.
[6] Ishimi, T., Miyaura, C., Jin, C.H., Akatsu, T., Abe, E., Nakamura, Y., Yamaguchi, Y., Yoshiki, S., Matsuda, T., Hirano, T., Kishimoto, T. and Suda, T. (1990) IL-6 is produced by

osteoblasts and induces bone resorption. J. Immunol. 145, 3297–3303.
[7] Helle, M., Brakenhoff, J.P.J., DeGroot, E.R. and Aarden, L.A. (1988) Interleukin-6 is involved in interleukin-1-induced activities. Eur. J. Immunol. 18, 957–959.
[8] Littlewood, A.J., Russil, J., Harvey, G.R., Hughes, D.E., Russel, R.G.G. and Gowen, M. (1991) The modulation of the expression of IL-6 and its receptor in human osteoblasts *in vitro*. Endocrinology 129, 1513–1520.
[9] Roodman, G.D. (1992) Interleukin-6: an osteotropic factor? J. Bone Miner. Res. 7, 475–478.
[10] Matsuno, M., Kozawa, O., Suzuki, A., Tokuda, H., Kaida, T., Matsuno, H., Niwa, M. and Uematsu, T. (1998) Involvement of protein kinase C activation in endothelin-1-induced secretion of interleukin-6 in osteoblast-like cells. Cell. Signal. 10, 107–111.
[11] Kawamura, H., Otsuka, T., Tokuda, H., Matsuno, H., Niwa, M., Matsui, N., Uematsu, T. and Kozawa, O. (1999) Involvement of p42/p44 MAP kinase in endothelin-1-induced interleukin-6 synthesis in osteoblast-like cells. Bone 24, 315–320.
[12] Widmann, C., Gibson, S., Jarpe, M.B. and Johnson, G.L. (1999) Mitogen-activated protein kinase: conservation of a three-kinase module from yeast to human. Physiol. Rev. 79, 143–180.
[13] Jankun, J., Selman, S.H., Swiercz, R. and Skrzypczak-Jankun, E. (1997) Why drinking green tea could prevent cancer. Nature 387, 561.
[14] Harbourne, J.B. and Williams, C.A. (2000) Advances in flavonoid research since 1992. Phytochemistry 55, 481–504.
[15] Delaisse, J.M., Eeckhout, Y. and Vaes, G. (1986) Inhibition of bone resorption in culture by (+)-catechin. Biochem. Pharmacol. 35, 3091–3094.
[16] Choi, E.-M. and Hwang, J.-K. (2003) Effects of (+)-catechin on the function of osteoblastic cells. Biol. Pharm. Bull. 26, 523–526.
[17] Sudo, H., Kodama, H., Amagai, Y., Yamamoto, S. and Kasai, S. (1983) *In vivo* differentiation and calcification in a new clonal osteogenic cell line derived from newborn mouse calvaria. J. Cell Biol. 96, 191–198.
[18] Kozawa, O., Tokuda, H., Miwa, M., Kotoyori, J. and Oiso, Y. (1992) Cross-talk regulation between cyclic AMP production and phosphoinositide hydrolysis induced by prostaglandin E_2 in osteoblast-like cells. Exp. Cell Res. 198, 130–134.
[19] Ishisaki, A., Tokuda, H., Yoshida, M., Hirade, K., Kunieda, K., Hatakeyama, D., Shibata, T. and Kozawa, O. (2004) Activation of p38 mitogen-activated protein kinase mediates thyroid hormone-stimulated osteocalcin synthesis in osteoblasts. Mol. Cell. Endocrinol. 214, 189–195.
[20] Robinson, R.J., Doty, S.B. and Cooper, R.R. (1973) Electron micrography of mammalian bone in: Biological Mineralization (Zipkin, I., Ed.), pp. 257–296, Academic Press, NY.
[21] Laemmli, U.K. (1970) Cleavage of structural proteins during the assembly of the head of bacteriophage T4. Nature 227, 680–685.
[22] Kato, K., Ito, H., Hasegawa, K., Inaguma, Y., Kozawa, O. and Asano, T. (1996) Modulation of the stress-induced synthesis of hsp27 and αB-crystallin by cyclic AMP in C6 glioma cells. J. Neurochem. 66, 946–950.
[23] Kawamura, H., Otsuka, T., Matsuno, H., Niwa, N., Matsui, N., Kato, K., Uematsu, T. and Kozawa, O. (1999) Endothelin-1 stimulates heat shock protein 27 induction in osteoblasts: involvement of p38 MAP kinase. Am. J. Physiol. 277, E1046–E1054.
[24] Wang, X., Tokuda, H., Hirade, K. and Kozawa, O. (2002) Stress-activated protein kinase/c-Jun N-terminal kinase (JNK) plays a part in endothelin-1-induced vascular endothelial growth factor synthesis in osteoblasts. J. Cell. Biochem. 87, 417–423.
[25] Cuenda, A., Rouse, J., Doza, Y.N., Meier, R., Cohen, P., Gallagher, T.F., Young, P.R. and Lee, J.C. (1995) SB203580 is a specific inhibitor of a MAP kinase homologue which is stimulated by cellular stresses and interleukin-1. FEBS Lett. 364, 229–233.
[26] Bennett, B.L., Sasaki, D.T., Murray, B.W., O'Leary, E.C., Sakata, S.T., Xu, W., Leisten, J.C., Motiwala, A., Pierce, S., Satoh, Y., Bhagwat, S.S., Manning, A.M. and Anderson, D.W. (2001) SP600125, an anthrapyrazolone inhibitor of Jun N-terminal Kinase. Proc. Natl. Acad. Sci. USA 98, 13681–13686.
[27] Nishizuka, Y. (1986) Studies and perspectives of protein kinase C. Science 233, 305–312.
[28] Kozawa, O., Suzuki, A., Tokuda, H. and Uematsu, T. (1997) Prostaglandin $F_{2\alpha}$ stimulates interleukin-6 via activation of PKC in osteoblast-like cells. Am. J. Physiol. 272, E208–E211.
[29] Tokuda, H., Harada, A., Hirade, K., Matsuno, H., Ito, H., Kato, K., Oiso, Y. and Kozawa, O. (2003) Incadronate amplifies prostaglandin $F_{2\alpha}$-induced vascular endothelial growth factor in osteoblasts: enhancement of MAP kinase activity. J. Biol. Chem. 278, 18930–18937.

Available online at www.sciencedirect.com
ScienceDirect
Biochemical and Biophysical Research Communications 362 (2007) 799–804
BBRC
www.elsevier.com/locate/ybbrc

Rho-kinase regulates endothelin-1-stimulated IL-6 synthesis via p38 MAP kinase in osteoblasts

Haruhiko Tokuda [a,b], Yoshiteru Hanai [a,b], Rie Matsushima-Nishiwaki [b], Junichi Yamauchi [b], Tomoaki Doi [b], Atsushi Harada [c], Shinji Takai [b], Osamu Kozawa [b,*]

[a] *Department of Clinical Laboratory, National Hospital for Geriatric Medicine, National Center for Geriatrics and Gerontology, Obu, Aichi 474-8511, Japan*
[b] *Department of Pharmacology, Gifu University Graduate School of Medicine, Gifu 501-1194, Japan*
[c] *Department of Functional Restoration, National Hospital for Geriatric Medicine, National Center for Geriatrics and Gerontology, Obu, Aichi 474-8511, Japan*

Received 2 August 2007
Available online 13 August 2007

Abstract

We have previously reported that endothelin-1 (ET-1) stimulates interleukin-6 (IL-6), a potent bone resorptive agent, through p44/p42 mitogen-activated protein (MAP) kinase and p38 MAP kinase in osteoblast-like MC3T3-E1 cells. In the present study, we investigated the involvement of Rho-kinase in the ET-1-stimulated IL-6 synthesis in MC3T3-E1 cells. ET-1 time-dependently induced the phosphorylation of myosin phosphatase targeting subunit (MYPT-1), a Rho-kinase substrate. Y27632, a specific inhibitor of Rho-kinase, significantly suppressed the IL-6 synthesis induced by ET-1 as well as the MYPT-1 phosphorylation. Fasudil, another inhibitor of Rho-kinase, reduced the ET-1-stimulated IL-6 synthesis. Y27632 as well as fasudil attenuated the ET-1-induced phosphorylation of p38 MAP kinase but not p44/p42 MAP kinase. These results strongly suggest that Rho-kinase regulates ET-1-stimulated IL-6 synthesis through p38 MAP kinase activation in osteoblasts.

Keywords: ET-1; Rho-kinase; IL-6; Osteoblast

It is well recognized that interleukin-6 (IL-6) is a multifunctional cytokine that has crucial effects on a wide range of functions such as promoting B cell differentiation, T cell activation, and inducing acute phase proteins [1–3]. The bone metabolism is regulated mainly by two functional cells, osteoblasts and osteoclasts, responsible for bone formation and bone resorption, respectively [4]. As for bone metabolism, IL-6 has been shown to stimulate bone resorption and promote osteoclast formation [2,3,5,6]. It has been reported that potent bone resorptive agents such as tumor necrosis factor-α and IL-1 stimulate IL-6 synthesis in osteoblasts [5,7,8]. Currently, evidence is accumulating that IL-6 secreted from osteoblasts plays a pivotal role as a downstream effector of bone resorptive agents.

Endothelin-1 (ET-1) is a potent vasoconstrictor produced by endothelial cells [9]. In bone metabolism, it is well recognized that ET-1 plays an important role in the regulation of bone metabolism and acts as a bone resorptive agent [10]. Accumulating evidence suggests that tumor-produced ET-1 mediates bone metastases by stimulating osteoblast proliferation and new bone formation [11]. As for intracellular signaling of ET-1 in osteoblasts, the activities of ET-1 are mediated via ET_A receptors and ET_B receptors [11]. We have shown that ET-1 activates phospholipase C and phospholipase D through ET_A receptors in osteoblast-like MC3T3-E1 cells [12]. Regarding about IL-6 synthesis, we have reported that ET-1 stimulates IL-6 synthesis via p44/p42 MAP kinase and p38 MAP kinase but not stress-activated protein kinase (SAPK)/c-Jun N terminal kinase (JNK) among the MAP kinase superfamily in these cells [13,14]. However, the exact mechanism

* Corresponding author. Fax: +81 58 230 6215.
E-mail address: okozawa@gifu-u.ac.jp (O. Kozawa).

0006-291X/$ - see front matter © 2007 Elsevier Inc. All rights reserved.
doi:10.1016/j.bbrc.2007.08.018

underlying ET-1-stimulated IL-6 synthesis in osteoblasts is not fully known.

Recent studies suggest that Rho and the down-stream effector, Rho-associated kinase (Rho-kinase) play important roles in a variety of cellular functions such as cell motility and smooth muscle contraction [15–17]. As for osteoblasts, it has been demonstrated that Rho and p38 MAP kinase are involved in the ET-1-induced expression of prostaglandin endoperoxide G/H synthase mRNA in osteoblasts [18]. In addition, Rho/Rho-kinase pathway reportedly stimulates osteoblast proliferation whereas it inhibits osteoblast differentiation [19]. However, the exact role of Rho-kinase in osteoblasts has not yet been fully clarified.

In the present study, we further investigated the exact mechanism behind ET-1-stimulated IL-6 synthesis in osteoblast-like MC3T3-E1 cells. We here show that Rho-kinase regulates ET-1-stimulated IL-6 synthesis through p38 MAP kinase activation in these cells.

Materials and methods

Materials. ET-1 and mouse IL-6 enzyme immunoassay (ELISA) kit were purchased from R&D Systems, Inc. (Minneapolis, MN). Y27632 was obtained from Calbiochem–Novabiochem Co. (LaJolla, CA). Hydroxyfasudil (fasudil) was from Sigma (St. Louis, MO). Phospho-specific MYPT-1 antibodies were purchased from Upstate (Lake Placid, NY). MYPT-1 antibodies were obtained form Santa Cruz Biotechnology, Inc. (Santa Cruz, CA). Phospho-specific p44/p42 MAP kinase antibodies, p44/p42 MAP kinase antibodies, phospho-specific p38 MAP kinase antibodies, and p38 MAP kinase antibodies were purchased from Cell Signaling, Inc. (Beverly, MA). ECL Western blotting detection system was purchased from Amersham Biosciences (Piscataway, NJ). Other materials and chemicals were obtained from commercial sources. Y27632 was dissolved in dimethyl sulfoxide (DMSO). The maximum concentration of DMSO was 0.1%, which did not affect the assay for IL-6 or Western blot analysis.

Cell culture. Cloned osteoblast-like MC3T3-E1 cells derived from newborn mouse calvaria [20] were maintained as previously described [21]. Briefly, the cells were cultured in α-minimum essential medium (α-MEM) containing 10% fetal calf serum (FCS) at 37 °C in a humidified atmosphere of 5% CO_2/95% air. The cells were seeded into 35- or 90-mm diameter dishes in α-MEM containing 10% FCS. After 5 days, the medium was exchanged for α-MEM containing 0.3% FCS. The cells were used for experiments after 48 h.

IL-6 assay. The cultured cells were stimulated by various doses of ET-1 in 1 ml of α-MEM containing 0.3% FCS for the indicated periods. When indicated, the cells were pretreated with various doses of Y27632 or fasudil for 60 min. The conditioned medium was collected at the end of the incubation, and the IL-6 concentration was measured by ELISA kit.

Western blot analysis. The cultured cells were pretreated with Y27632 or fasudil for 60 min, and then stimulated by ET-1 in α-MEM containing 0.3% FCS for the indicated periods. The cells were washed twice with phosphate-buffered saline and then lysed, homogenized, and sonicated in a lysis buffer containing 62.5 mM Tris/HCl, pH 6.8, 2% sodium dodecyl sulfate (SDS), 50 mM dithiothreitol and 10% glycerol. The cytosolic fraction was collected as a supernatant after centrifugation at 125,000*g* for 10 min at 4 °C. SDS–polyacrylamide gel electrophoresis (PAGE) was performed by Laemmli [22] in 10% polyacrylamide gel. Western blotting analysis was performed as described previously [23] by using phospho-specific MYPT-1 antibodies, MYPT-1 antibodies, phospho-specific p44/p42 MAP kinase antibodies, p44/p42 MAP kinase antibodies, phospho-specific p38 MAP kinase antibodies or p38 MAP kinase antibodies, with peroxidase-labeled antibodies raised in goat against rabbit IgG being used as second antibodies. Peroxidase activity on the PVDF sheet was visualized on X-ray film by means of the ECL Western blotting detection system.

Determination. The absorbance of enzyme immunoassay samples was measured at 450 nm with EL 340 Bio Kinetic Reader (Bio-Tek Instruments, Inc., Winooski, VT). The densitometric analysis was performed using Molecular Analyst/Macintosh (Bio-Rad Laboratories, Hercules, CA).

Statistical analysis. The data were analyzed by ANOVA followed by the Bonferroni method for multiple comparisons between pairs, and a $p < 0.05$ was considered significant. All data are presented as the means ± SEM of triplicate determinations. Each experiment was repeated three times with similar results.

Results

Effects of ET-1 on the phosphorylation of MYPT-1 in MC3T3-E1 cells

It is well known that myosin phosphatase targeting subunit (MYPT-1), which is a component of myosin phosphatase, is a down-stream substrate of Rho-kinase [15,24]. To investigate whether ET-1 activates Rho-kinase in osteoblast-like MC3T3-E1 cells, we examined the effect of ET-1 on the phosphorylation of MYPT-1. ET-1 significantly induced the phosphorylation of MYPT-1 in a time-dependent manner (Fig. 1A). The effect of ET-1 on the MYPT-1 phosphorylation reached its peak within 2 min and decreased thereafter (Fig. 1A).

We found that Y27632, a specific inhibitor of Rho-kinase [16], markedly suppressed the ET-1-induced phosphorylation levels of MYPT-1 (Fig. 1B). Additionally, the phosphorylation levels of MYPT-1 induced by ET-1 were attenuated by fasudil, another inhibitor of Rho-kinase [16] (data not shown).

Effects of Y27632 or fasudil on the ET-1-stimulated IL-6 synthesis in MC3T3-E1 cells

We previously showed that ET-1 stimulates IL-6 synthesis in osteoblast-like MC3T3-E1 cells [13]. In order to investigate whether or not Rho-kinase is involved in the ET-1-induced synthesis of IL-6 in MC3T3-E1 cells, we next examined the effect of Y27632 on the synthesis of IL-6 induced by ET-1. Y27632, which alone failed to affect the IL-6 levels, significantly suppressed the ET-1-induced synthesis of IL-6 (Fig. 2). The inhibitory effect of Y27632 was dose-dependent in the range between 0.1 and 10 μM. Y27632 at 10 μM caused approximately 90% inhibition in the ET-1-effect.

Fasudil as well as Y27632 reduced the ET-1-stimulated IL-6 synthesis in these cells (Table 1). The effect of fasudil on the IL-6 synthesis was dose-dependent in the range between 0.3 and 3 μM. Fasudil (3 μM) caused approximately 70% inhibition in the ET-1-effect.

Effect of Y27632 on the ET-1-induced phosphorylation of p44/p42 MAP kinase in MC3T3-E1 cells

It is generally recognized that three MAP kinases, p44/p42 MAP kinase, p38 MAP kinase and SAPK/JNK are known as central elements used by mammalian cells to

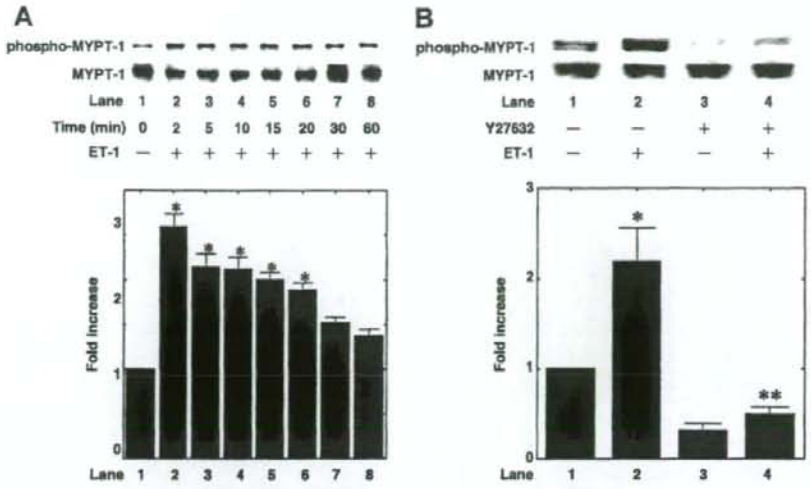

Fig. 1. Effect of ET-1 on the phosphorylation of MYPT-1 and effect of Y27632 on the ET-1-induced phosphorylation of MYPT-1 in MC3T3-E1 cells. (A) The cultured cells were stimulated by 0.1 μM ET-1 for the indicated periods. (B) The cultured cells were pretreated with 10 μM Y27632 or vehicle for 60 min, and then stimulated by 0.1 μM ET-1 or vehicle for 2 min. The extracts of cells were subjected to SDS–PAGE with subsequent Western blotting analysis with antibodies against phospho-specific MYPT-1 or MYPT-1. The histogram shows quantitative representations of the levels of ET-1-induced phosphorylation obtained from laser densitometric analysis of three independent experiments. Each value represents the mean ± SEM of triplicate determinations. Similar results were obtained with two additional and different cell preparations. $^{*}p < 0.05$, compared to the value of control. $^{**}p < 0.05$, compared to the value of ET-1 alone.

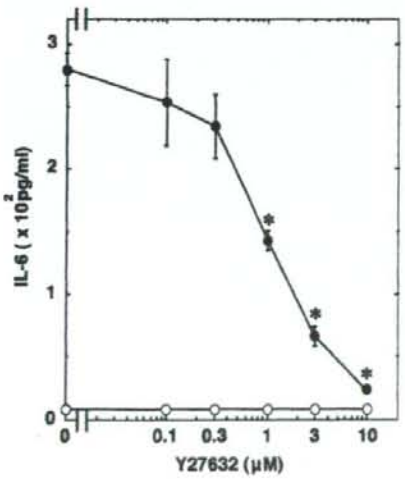

Fig. 2. Effect of Y27632 on the ET-1-induced IL-6 synthesis in MC3T3-E1 cells. The cultured cells were pretreated with various doses of Y27632 for 60 min, and then stimulated by 0.1 μM ET-1 or vehicle for 48 h. Each value represents the mean ± SEM of triplicate determinations. Similar results were obtained with two additional and different cell preparations. $^{*}p < 0.05$, compared to the value of ET-1 alone.

Table 1
Effect of fasudil on the ET-1-stimulated IL-6 synthesis in MC3T3-E1 cells

Fasudil (μM)	ET-1	IL-6 (pg/ml)
0	–	<7.8
0	+	287 ± 16*
0.3	–	<7.8
0.3	+	261 ± 6
1	–	<7.8
1	+	171 ± 5**
3	–	<7.8
3	+	70 ± 5**

The cultured cells were pretreated with various doses of fasudil for 60 min, and then stimulated by 0.1 μM ET-1 or vehicle for 48 h. Each value represents the mean ± SEM of triplicate determinations. Similar results were obtained with two additional and different cell preparations.
* $p < 0.05$, compared to the control.
** $p < 0.05$, compared to the value of ET-1 alone.

transduce the various messages of a variety of agonists [25]. In our previous studies [13,14], we have shown that ET-1 stimulates IL-6 synthesis via p44/p42 MAP kinase and p38 MAP kinase but not SAPK/JNK among the MAP kinase superfamily in osteoblast-like MC3T3-E1 cells. In order to investigate whether Rho-kinase-effect on the ET-1-stimulated IL-6 synthesis is dependent upon the activation of p44/p42 MAP kinase or p38 MAP kinase in MC3T3-E1 cells, we next examined the effect of Y27632 on the phosphorylation of p44/p42 MAP kinase by ET-1. However, Y27632 failed to affect the ET-1-induced phosphorylation of p44/p42 MAP kinase (Fig. 3).

Effects of Y27632 or fasudil on the ET-1-induced phosphorylation of p38 MAP kinase in MC3T3-E1 cells

In addition, we examined effect of Y27632 on the ET-1-induced phosphorylation of p38 MAP kinase in MC3T3-E1 cells. Y27632, which itself had little effect on

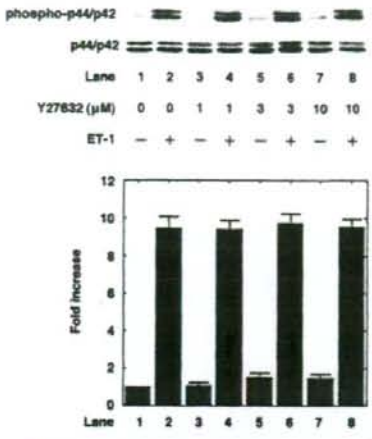

Fig. 3. Effect of Y27632 on the ET-1-induced phosphorylation of p44/p42 MAP kinase in MC3T3-E1 cells. The cultured cells were pretreated with various doses of Y27632 for 60 min, and then stimulated by 0.1 μM ET-1 or vehicle for 5 min. The extracts of cells were subjected to SDS–PAGE with subsequent Western blotting analysis with antibodies against phospho-specific p44/p42 MAP kinase or p44/p42 MAP kinase. The histogram shows quantitative representations of the levels of ET-1-induced phosphorylation obtained from laser densitometric analysis of three independent experiments. Each value represents the mean ± SEM of triplicate determinations. Similar results were obtained with two additional and different cell preparations.

the phosphorylation of p38 MAP kinase, markedly suppressed the ET-1-induced phosphorylation of p38 MAP kinase (Fig. 4A). The Y27632-effect on the phosphorylation levels was dose-dependent in the range between 1 and 10 μM. Y27632 (10 μM) caused about 80% inhibition in the ET-1-effect.

Fasudil attenuated the ET-1-induced levels of phosphorylated-p38 MAP kinase (Fig. 4B). The inhibitory effect of fasudil was dose-dependent in the range between 1 and 10 μM. Fasudil (10 μM) caused approximately 70% inhibition in the ET-1-effect.

Discussion

In the present study, we found that ET-1 time-dependently induced the phosphorylation of MYPT-1 in osteoblast-like MC3T3-E1 cells, using phospho-specific MYPT-1 (Thr850) antibodies. It is generally recognized that MYPT is a myosin-binding subunit of myosin phosphatase, which regulates the interaction of actin and myosin, and a downstream target of Rho-kinase [15,24]. In addition, we found that Rho-kinase inhibitors [16] such as Y27632 and fasudil truly reduced the ET-1-induced phosphorylation levels of MYPT-1. Taking our findings into account, it is most likely that ET-1 stimulates the activation of Rho-kinase in osteoblast-like MC3T3-E1 cells.

We next investigated whether Rho-kinase functions in the ET-1-stimulated IL-6 synthesis or not in osteoblast-like MC3T3-E1 cells. The ET-1-stimulated synthesis of IL-6 was significantly suppressed by Y27632, a specific inhibitor of Rho-kinase [16]. We confirmed that the Rho-kinase inhibitor truly reduced the ET-1-induced phosphorylation levels of MYPT-1. It seems that the activated Rho-kinase acts as a positive regulator in the IL-6 synthesis by ET-1 in osteoblast-like MC3T3-E1 cells. In addition, the ET-1-

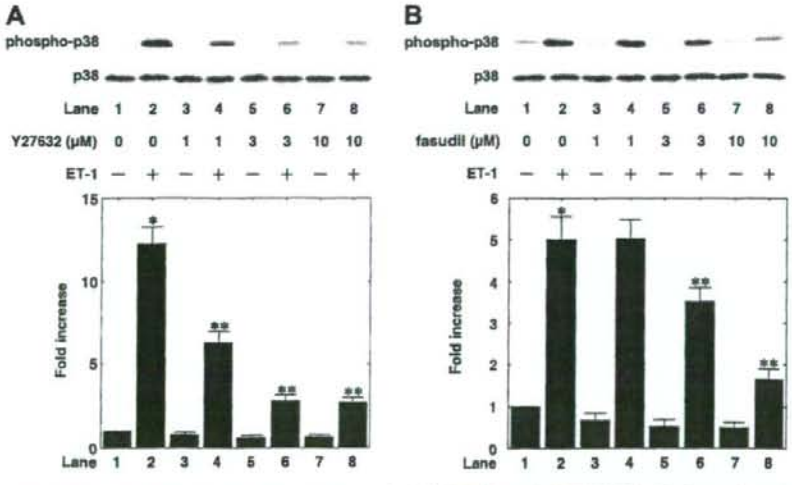

Fig. 4. Effects of Y27632 or fasudil on the ET-1-induced phosphorylation of p38 MAP kinase in MC3T3-E1 cells. The cultured cells were pretreated with various doses of Y27632 (A) or fasudil (B) for 60 min, and then stimulated by 0.1 μM ET-1 or vehicle for 20 min. The extracts of cells were subjected to SDS–PAGE with subsequent Western blotting analysis with antibodies against phospho-specific p38 MAP kinase or p38 MAP kinase. The histogram shows quantitative representations of the levels of ET-1-induced phosphorylation obtained from laser densitometric analysis of three independent experiments. Each value represents the mean ± SEM of triplicate determinations. Similar results were obtained with two additional and different cell preparations. $^{*}p < 0.05$, compared to the control. $^{**}p < 0.05$, compared to the value of ET-1 alone.

stimulated IL-6 synthesis as well as the phosphorylated levels of MYPT-1 was inhibited by fasudil, another Rho-kinase inhibitor [16]. Therefore, based on our results, it is most likely that ET-1 activates Rho-kinase, resulting in up-regulation of IL-6 synthesis in osteoblast-like MC3T3-E1 cells.

Regarding about IL-6 synthesis, we have previously demonstrated that the ET-1 stimulated IL-6 synthesis is mediated by activation of p44/p42 MAP kinase and p38 MAP kinase but not SAPK/JNK among the MAP kinase superfamily in osteoblast-like MC3T3-E1 cells [13,14]. Additionally, we investigated the relationship between Rho-kinase and these MAP kinases in the IL-6 synthesis in MC3T3-E1 cells. However, Y27632 failed to affect the ET-1-induced phosphorylation levels of p44/p42 MAP kinase. Therefore, it seems unlikely that Rho-kinase affects the ET-1-stimulated IL-6 synthesis through the modulation of p44/p42 MAP kinase in osteoblast-like MC3T3-E1 cells. On the contrary, the ET-1-induced phosphorylation levels of p38 MAP kinase were significantly suppressed by Y27632 and fasudil. These results suggest that Rho-kinase regulates the ET-1-stimulated IL-6 synthesis via p38 MAP kinase. In the present study, the maximum effect on the phosphorylation of MYPT-1, a well-known downstream target of Rho-kinase [15], was observed within 2 min after the ET-1 stimulation. In our previous study [26], we have shown that the phosphorylation of p38 MAP kinase reach the peak at 20 min after the stimulation of ET-1 in MC3T3-E1 cells. The time course of the phosphorylation of MYPT-1 stimulated by ET-1 seems to be faster than that of p38 MAP kinase, in turn, ET-1-induced activation of p38 MAP kinase subsequently occurs after the Rho-kinase activation. Taking our findings into account as a whole, it is most likely that Rho-kinase acts at a point upstream from p38 MAP kinase in the ET-1-induced IL-6 synthesis in osteoblast-like MC3T3-E1 cells.

Rho-kinase is currently recognized to play a pivotal role in various cellular functions, especially vascular smooth muscle contraction [15,16]. In bone metabolism, it has been reported that the Rho-kinase pathway acts as a negative regulator of osteoblast differentiation and induces osteoblast proliferation [19]. Our present results indicate that Rho-kinase activation in osteoblasts has an important role in the control of the production of IL-6, one of the key regulators of bone metabolism. It is well known that IL-6 produced by osteoblasts is a potent bone resorptive agent and induces osteoclast formation [3,5]. In addition, it is recognized that ET-1 acts as a bone resorptive agent in bone metabolism [10]. Evidence is recently accumulating that tumor cells produces ET-1 which mediates bone metastasis by stimulating the proliferation of osteoblasts and new bone formation [11]. Therefore, our present findings lead us to speculate that ET-1-activated Rho-kinase acts as a positive regulator of bone resorption via the fine tuning of local cytokine network. Therefore, the Rho-kinase pathway in osteoblasts might be considered to be a new candidate as a molecular therapeutic target of bone resorption and osteoblastic bone metastases due to breast or prostate cancer. The pathophysiological significance of regulatory mechanism by Rho-kinase in osteoblasts remains still unclear. Further investigation is necessary to clarify the exact role of Rho-kinase in osteoblasts.

In conclusion, our results strongly suggest that Rho-kinase regulates the ET-1-stimulated IL-6 synthesis at a point upstream from p38 MAP kinase in osteoblasts.

Acknowledgments

We are very grateful to Yoko Kawamura and Seiko Sakakibara for their skillful technical assistance. This investigation was supported in part by Grant-in-Aid for Scientific Research (16590873 and 16591482) for the Ministry of Education, Science, Sports and Culture of Japan, the Research Grants for Longevity Sciences (15A-1 and 15C-2), Research Grant on Proteomics and Research Grant on Longevity Sciences from the Ministry of Health, Labour and Welfare of Japan.

References

[1] S. Akira, T. Taga, T. Kishimoto, Interleukin-6 in biology and medicine, Adv. Immunol. 54 (1993) 1–78.
[2] D. Heymann, A.V. Rousselle, gp130 Cytokine family and bone cells, Cytokine 12 (2000) 1455–1468.
[3] S. Kwan Tat, M. Padrines, S. Theoleyre, D. Heymann, Y. Fortun, IL-6 is produced by osteoblasts and induces bone resorption, Cytokine Growth Factor Rev. 15 (2004) 49–60.
[4] P.J. Nijweide, E.H. Burger, J.H.M. Feyen, Cells of bone: proliferation, differentiation, and hormonal regulation, Physiol. Rev. 86 (1986) 855–886.
[5] Y. Ishimi, C. Miyaura, C.H. Jin, T. Akatsu, F. Abe, Y. Nakamura, Y. Yamaguchi, S. Yoshiki, T. Matsuda, T. Hirano, T. Kishimoto, T. Suda, IL-6 is produced by osteoblasts and induces bone resorption, J. Immunol. 145 (1990) 3297–3303.
[6] G.D. Roodman, Interleukin-6: an osteotropic factor? J. Bone Miner. Res. 7 (1992) 475–478.
[7] M. Helle, J.P.J. Brakenhoff, E.R. DeGroot, L.A. Aarden, Interleukin 6 is involved in interleukin 1-induced activities, Eur. J. Immunol. 18 (1998) 957–959.
[8] A.J. Littlewood, J. Russil, G.R. Harvey, D.E. Hughes, R.G.G. Russel, M. Gowen, The modulation of the expression of IL-6 and its receptor in human osteoblasts in vitro, Endocrinology 129 (1991) 1513–1520.
[9] T. Miyauchi, T. Masaki, Pathophysiology of endothelin in the cardiovascular system, Annu. Rev. Physiol. 61 (1999) 391–415.
[10] P.H. Stern, A. Tatrai, D.E. Semler, S.K. Lee, P. Lakatos, P.J. Strieleman, G. Tarjan, J.L. Sanders, Endothelin receptors, second messengers, and actions in bone, J. Nutr. 125 (1995) 2028S–2032S.
[11] T.A. Guise, J.J. Yin, K.S. Mohammad, Role of endothelin-1 in osteoblastic bone metastases, Cancer 97 (2003) 779–784.
[12] A. Suzuki, J. Shinoda, Y. Watanabe-Tomita, N. Ozaki, Y. Oiso, O. Kozawa, ET_A receptor mediates the signalling of endothelin-1 in osteoblast-like cells, Bone 21 (1997) 143–146.
[13] H. Kawamura, T. Otsuka, H. Tokuda, H. Matsuno, N. Niwa, N. Matsui, T. Uematsu, O. Kozawa, Involvement of p42/p44 MAP kinase in endothelin-1-induced interleukin-6 synthesis in osteoblast-like cells, Bone 24 (1999) 315–320.
[14] H. Tokuda, S. Takai, Y. Hanai, R. Matsushima-Nishiwaki, T. Hosoi, A. Harada, T. Ohta, O. Kozawa, (−)-Epigallocatechin gallate suppresses endothelin-1-induced interleukin-6 synthesis in osteoblasts: inhibition of p44/p42 MAP kinase activation, FEBS Lett. 581 (2007) 1311–1316.

[15] Y. Fukata, M. Amano, K. Kaibuchi, Rho–Rho-kinase pathway in smooth muscle contraction and cytoskeletal reorganization of non-muscle cells, Trends Pharmacol. Sci. 22 (2001) 32–39.
[16] H. Shimokawa, M. Rashid, Development of Rho-kinase inhibitors for cardiovascular medicine, Trends Pharmacol. Sci. 28 (2007) 296–302.
[17] K. Riento, A.J. Ridley, Rocks: multifunctional kinases in cell behaviour, Nat. Rev. Mol. Cell Biol. 4 (2003) 446–456.
[18] W. Windischhofer, D. Zach, G. Fauler, G. Raspotnig, H. Kofeler, H.J. Leis, Involvement of Rho and p38 MAPK in endothelin-1-induced expression of PGHS-2 mRNA in osteoblast-like cells, J. Bone Miner. Res. 17 (2002) 1774–1784.
[19] D. Harmey, G. Stenbeck, C.D. Nobes, A.J. Lax, A.E. Grigoriadis, Regulation of osteoblast differentiation by Pasteurella multocida toxin (PMT): a role for Rho GTPase in bone formation, J. Bone Miner. Res. 19 (2004) 661–670.
[20] H. Sudo, H. Kodama, Y. Amagai, S. Yamamoto, S. Kasai, In vitro differentiation and calcification in a new clonal osteogenic cell line derived from newborn mouse calvaria, J. Cell Biol. 96 (1983) 191–198.
[21] O. Kozawa, H. Tokuda, M. Miwa, J. Kotoyori, Y. Oiso, Cross-talk regulation between cyclic AMP production and phosphoinositide hydrolysis induced by prostaglandin E_2 in osteoblast-like cells, Exp. Cell Res. 198 (1992) 130–134.
[22] U.K. Laemmli, Cleavage of structural proteins during the assembly of the head of bacteriophage T4, Nature 227 (1970) 680–685.
[23] K. Kato, H. Ito, K. Hasegawa, Y. Inaguma, O. Kozawa, T. Asano, Modulation of the stress-induced synthesis of hsp27 and alpha B-crystallin by cyclic AMP in C6 rat glioma cells, J. Neurochem. 66 (1996) 946–950.
[24] M. Ito, T. Nakano, F. Erdodi, D.J. Hartshorne, Myosin phosphatase: structure, regulation and function, Mol. Cell. Biochem. 259 (2004) 197–209.
[25] C. Widmann, S. Gibson, M.B. Jarpe, G.L. Johnson, Mitogen-activated protein kinase: conservation of a three-kinase module from yeast to human, Physiol. Rev. 79 (1999) 143–180.
[26] H. Kawamura, T. Otsuka, H. Matsuno, M. Niwa, N. Matsui, K. Kato, T. Uematsu, O. Kozawa, Endothelin-1 stimulates heat shock protein 27 induction in osteoblasts: involvement of p38 MAP kinase, Am. J. Physiol. 277 (1999) E1046–E1054.

Ann Nucl Med (2007) 21:361–365
DOI 10.1007/s12149-007-0028-9

CASE REPORT

Metastasis of the gastrointestinal tract: FDG-PET imaging

**Kazumasa Hayasaka · Takashi Nihashi
Toshihiro Matsuura · Tetsuya Yagi
Kazumitsu Nakashima · Yasuji Kawabata · Kengo Ito
Takashi Katoh · Keita Sakata · Atsushi Harada**

Received: 6 December 2006 / Accepted: 23 March 2007

Abstract We assess the usefulness of F-18-fluoro-deoxyglucose (FDG) positron emission tomography (PET) in the evaluation of gastrointestinal metastases. Four cases (five lesions) in which metastases from three lung cancers and one malignant fibrous histiocytoma (MFH) of the femur were found in the gastrointestinal tract were reviewed (men/women 3:1, age 63–78 years, mean 72 years). The five lesions were duodenal, jejunal metastasis, and two stomach metastases from lung carcinoma, and rectal metastasis from MFH of the femur. FDG-PET was unable to detect small masses, but it was able to detect unforeseen lesions such as gastrointestinal metastases because FDG-PET is a whole-body scan in a single-operation examination. FDG-PET imaging provided valuable information for the diagnosis of gastrointestinal metastasis.

Keywords F18-FDG-PET · Gastrointestinal tract · Secondary neoplasms

K. Hayasaka (✉) · T. Nihashi
Department of Radiology, National Center for Geriatrics and Gerontology, 36-3 Gengo, Morioka-machi, Obu 474-8511, Japan
e-mail: ckv37824@mopera.ne.jp

T. Matsuura
Department of Gastroenterology, National Center for Geriatrics and Gerontology, Obu, Japan

T. Yagi · K. Nakashima
Department of Internal Medicine, National Center for Geriatrics and Gerontology, Obu, Japan

Y. Kawabata
Department of Surgery, National Center for Geriatrics and Gerontology, Obu, Japan

K. Ito · T. Katoh
Department of Brain Science and Molecular Imaging, National Center for Geriatrics and Gerontology, Obu, Japan

K. Sakata
Department of Pathology, National Center for Geriatrics and Gerontology, Obu, Japan

A. Harada
Department of Orthopedics, National Center for Geriatrics and Gerontology, Obu, Japan

Introduction

Gastrointestinal metastases are rarely detected early, but often are detected incidentally at autopsy [1, 2]. These metastases are relatively asymptomatic and rarely pose clinical problems but sometimes manifest themselves by serious complications such as gastrointestinal perforation and intussusception [3]. From this point of view, it is important to diagnose gastrointestinal metastasis before such serious complications arise.

The useful clinical application of F-18-fluoro-deoxyglucose (FDG) positron emission tomography (PET) in the diagnosis of tumors has been already reported [4, 5]. Because studies have reported on FDG uptake in primary gastric cancer and primary colorectal cancer [6–8], metastatic tumors of the gastrointestinal tract are also expected to take up FDG. FDG-PET can detect gastrointestinal metastases, allowing their diagnosis before the development of serious complications.

The PET database of the National Center Hospital for Geriatric Medicine was retrospectively searched for all patients who had undergone a whole-body FDG-PET scan for tumor detection during the period of July 1996 to June 2006. A total of 308 subjects were studied for tumor detection. Of these, four cases (five lesions) in

Table 1 Clinical and fluoro-deoxyglucose positron emission tomography data

Case	Age/sex	Symptom	Metastatic site	Primary site	Pathology	Mean SUV in the early scan	Mean SUV in the delayed scan	Tumor size (cm)
1	78/M	Nausea	Duodenum	Lung	Adenocarcinoma	8.5	9.2	3
			Jejunum		Adenocarcinoma	5.8	8.1	2
2	76/M	Bloody stool	Rectum	Femoral bone	MFH	5.1	ND	4.5
3	63/M	Abdominal discomfort	Stomach	Lung	SCC	7.9	9.1	3
4	72/F	Epigastralgia	Stomach	Lung	Adenocarcinoma	5.9	ND	3

SUV standardized uptake value, *ND* not done, *MFH* malignant fibrous histiocytoma, *SCC* squamous cell carcinoma, *M* male, *F* female

which metastases were found in the gastrointestinal tract were reviewed (men/women 3:1, age 63–78 years, mean 72 years).

FDG-PET imaging was performed as follows: an ECAT EXACT HR 47 PET camera (Siemens/CTI) was used, and imaging was performed using 3D acquisition at 60 min (all patients) and 120 min (two patients) after the intravenous administration of 250 MBq F-18-FDG. The collected data were reconstructed in a 128 × 128 pixel image matrix. The tissue attenuation of annihilation photons was corrected by transmission scans using rotating $^{68}Ge/^{68}Ga$ line sources. Six bed positions of the body trunk were used, which covered areas from the neck to the pelvis. The total time for one bed position was 6 min, with a transmission scan of 2 min and an emission scan of 4 min. The patient fasted for at least 6 h prior to the examination. Normal glucose level was confirmed prior to the PET scan. Regional FDG uptake in the affected area was expressed as standardized uptake value.

Table 1 summarizes the clinical and FDG-PET data of the four cases.

Case reports

Case 1

A 78-year-old man who had been diagnosed with lung adenocarcinoma by transbronchial lung biopsy received chemotherapy and achieved complete remission (CR). After 6 months, he sought medical attention with a chief complaint of vomiting. Computed tomography (CT) was performed and revealed a thickened wall and masses in the duodenum and jejunum (Fig. 1a). After 5 days, FDG-PET was performed for restaging and for the detection of metastatic lesions. FDG-PET showed hypermetabolism in the duodenum and jejunum (Fig. 1b), and in delayed scan showed increased uptake in the duodenum and jejunum. Gastroduodenoscopy showed a submucosal tumor in the duodenum. Metastatic adenocarcinoma was diagnosed by biopsy from the duodenum (Fig. 1c).

Case 2

A 76-year-old man who underwent surgery for malignant fibrous histiocytoma (MFH) of the femoral bone experienced gastrointestinal bleeding after 7 months, and was hospitalized. Hematological examination detected anemia, but no abnormality was found in the blood chemistry on admission. FDG-PET was performed to investigate metastasis. FDG-PET revealed hypermetabolic areas in the regions above the rectum (Fig. 2a), whereas colonoscopy showed a submucosal tumor in the rectum. The tumors were diagnosed as metastases from MFH of the femoral bone, and tumorectomy of the rectum was performed. The diagnosis was established histopathologically(Fig. 2b).

Case 3

A 63-year-old man had undergone surgery for squamous cell carcinoma (SCC) in the right upper lung field. Five years later, he had abdominal discomfort and a high carcinoembryonic (CEA) level (28.5 ng/ml). CT showed a round thickened wall in the stomach (Fig. 3a). After 10 days, FDG-PET performed for the detection of recurrent and metastatic lesions revealed hypermetabolism in the stomach (Fig. 3b). Gastroduodenoscopy showed a submucosal tumor of the stomach. Gastrectomy was performed and the tumor was histopathologically diagnosed as metastatic poorly differentiated SCC of the stomach (Fig. 3c).

Discussion

Metastatic tumors of the gastrointestinal tract rarely present with symptoms peculiar to these tumors, and are

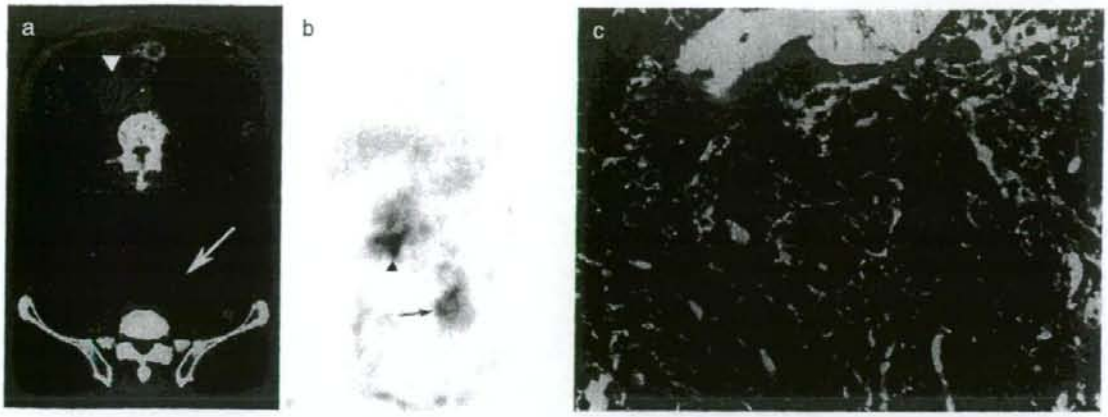

Fig. 1 Computed tomography revealed thickened wall and masses in the duodenum (*arrowhead*) and jejunum (*arrow*) (**a**). Fluorodeoxyglucose positron emission tomography (FDG-PET) showed hypermetabolism in the duodenum (*arrowhead*) and jejunum (*arrow*) (**b**). Pathology by biopsies from the duodenum (hematoxylin-eosin, H&E) (**c**) revealed findings similar to those of pathological tissue of lung carcinoma obtained by biopsy from transbronchial lung biopsy, confirming a metastatic adenocarcinoma

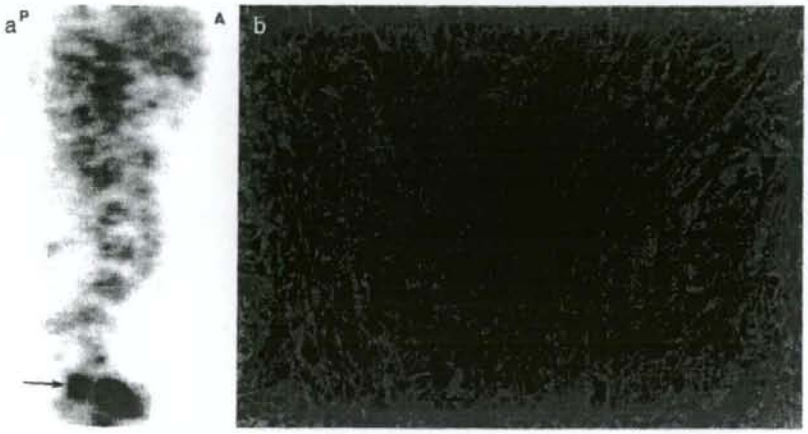

Fig. 2 FDG-PET showing hypermetabolism in the rectum (*arrowhead*) (**a**). The mean standardized uptake value calculated by FDG-PET was 5.1 for the rectal tumor. Pathology by surgery from the rectum (H&E) confirmed a metastatic malignant fibrous histiocytoma (**b**)

rarely detected before the development of serious complications such as acute abdomen. Abrams et al. [1] reported that they found metastases to the stomach and intestine and esophagus in 20% and 3.1% of the 1000 autopsies of cancer patients. Meyers and McSweeney [9] reported that the primary lesions of metastatic tumors of the gastrointestinal tract in 40 clinical patients were malignant melanoma (57%), breast cancer (25%), and lung cancer (18%), indicating that malignant melanoma is the most frequent, followed by breast and lung cancers. Metastatic tumors of the gastrointestinal tract often present with abdominal pain, vomiting, anemia, and melena, and often have metastasized to other organs at the time of detection [10]. Sometimes they first present with acute abdomen such as intestinal perforation, intussusception, intestinal obstruction, or massive gastrointestinal bleeding [3, 11, 12]. Hence, it is desirable to detect metastatic tumors of the gastrointestinal tract before the development of such serious complications. The role and potential value of FDG-PET scanning in certain neoplasms have been widely investigated in recent years [4, 5]. These investigations have been performed predominantly on lung, colorectal, breast, and brain tumors. More recently, the role of FDG-PET has been in upper gastrointestinal neoplasms [4–6, 13, 14]. The usefulness of FDG-PET in recurrent tumors other than these primary tumors of the esophagus, stomach, and intestine has also reported [15, 16], encouraging expectations that FDG-PET will also be useful for the detection of metastatic tumors of the gastrointestinal tract. A few